PHILOSOPHICAL TRANSACTIONS OF THE ROYAL SOCIETY B

Phil. Trans. R. Soc. B (2012) **367**, 583–600
doi:10.1098/rstb.2011.0261

Research

Evolution of C_4 plants: a new hypothesis for an interaction of CO_2 and water relations mediated by plant hydraulics

Colin P. Osborne[1,*] **and Lawren Sack**[2]

[1]*Department of Animal and Plant Sciences, University of Sheffield, Sheffield S10 2TN, UK*
[2]*UCLA Ecology and Evolutionary Biology, 621 Charles E. Young Drive South, Box 951606, Los Angeles, CA 90095-1606, USA*

C_4 photosynthesis has evolved more than 60 times as a carbon-concentrating mechanism to augment the ancestral C_3 photosynthetic pathway. The rate and the efficiency of photosynthesis are greater in the C_4 than C_3 type under atmospheric CO_2 depletion, high light and temperature, suggesting these factors as important selective agents. This hypothesis is consistent with comparative analyses of grasses, which indicate repeated evolutionary transitions from shaded forest to open habitats. However, such environmental transitions also impact strongly on plant–water relations. We hypothesize that excessive demand for water transport associated with low CO_2, high light and temperature would have selected for C_4 photosynthesis not only to increase the efficiency and rate of photosynthesis, but also as a water-conserving mechanism. Our proposal is supported by evidence from the literature and physiological models. The C_4 pathway allows high rates of photosynthesis at low stomatal conductance, even given low atmospheric CO_2. The resultant decrease in transpiration protects the hydraulic system, allowing stomata to remain open and photosynthesis to be sustained for longer under drying atmospheric and soil conditions. The evolution of C_4 photosynthesis therefore simultaneously improved plant carbon and water relations, conferring strong benefits as atmospheric CO_2 declined and ecological demand for water rose.

Keywords: C_4 photosynthesis; C_3 photosynthesis; atmospheric CO_2; plant evolution; drought; hydraulics

1. PHOTOSYNTHETIC CONSERVATISM AND DIVERSITY

Photosynthesis has evolved only once, and every photoautotrophic organism on Earth uses the same 'C_3 pathway' [1]. This biochemical cycle employs the enzyme Rubisco to fix CO_2 into a five-carbon acceptor molecule, producing three-carbon organic acids, upon which ATP and NADPH produced from the light reactions are deployed to generate sugars and to regenerate the acceptor molecule. The pigments and proteins involved in C_3 photosynthesis are highly conserved across photosynthetic organisms, and this pathway operates unmodified in the majority of species, termed 'C_3 plants'. However, the basic C_3 pathway has also been augmented by carbon-concentrating mechanisms (CCMs) in multiple lineages, many of which evolved during the Early Neogene following a massive depletion of atmospheric CO_2 [2–5].

'C_4 photosynthesis' is a collective term for CCMs which initially fix carbon into four-carbon organic acids via the enzyme phosphoenolpyruvate carboxylase (PEPC) [6], and then liberate CO_2 from these C_4 acids to feed the C_3 pathway within a compartment of the cell or leaf [7,8] (figure 1*a*). The compartment is isolated from the atmosphere and resists CO_2-leakage, so that CO_2 is enriched at the active site of Rubisco [12] (figure 1*a*). Coordination of C_4 and C_3 biochemical pathways requires complex changes to metabolism, and the compartmentation of these pathways usually relies on a specialized leaf anatomy (figure 1*b*). C_4 photosynthesis is therefore a complex trait based on the transcriptional regulation of hundreds of genes [13], coupled with post-transcriptional regulation [14] and the adaptation of protein-coding sequences [15].

Despite the complexity of C_4 photosynthesis, it has been recorded in more than 60 plant lineages [16]. This striking evolutionary convergence probably arises because the pathway is constructed from numerous pre-existing gene networks [17], and altered levels and patterns of expression of enzymes that are already present in C_3 leaves [18–20]. Many of the known C_4 lineages occur in clusters, suggesting that they share early steps on the evolutionary trajectory towards C_4 photosynthesis, taking an independent path only during later stages of the process [21].

In recent years, evidence from genomics, molecular genetics, physiology, ecology, biogeography,

* Author for correspondence (c.p.osborne@sheffield.ac.uk).

Electronic supplementary material is available at http://dx.doi.org/10.1098/rstb.2011.0261 or via http://rstb.royalsocietypublishing.org.

One contribution of 12 to a Theme Issue 'Atmospheric CO_2 and the evolution of photosynthetic eukaryotes: from enzymes to ecosystems'.

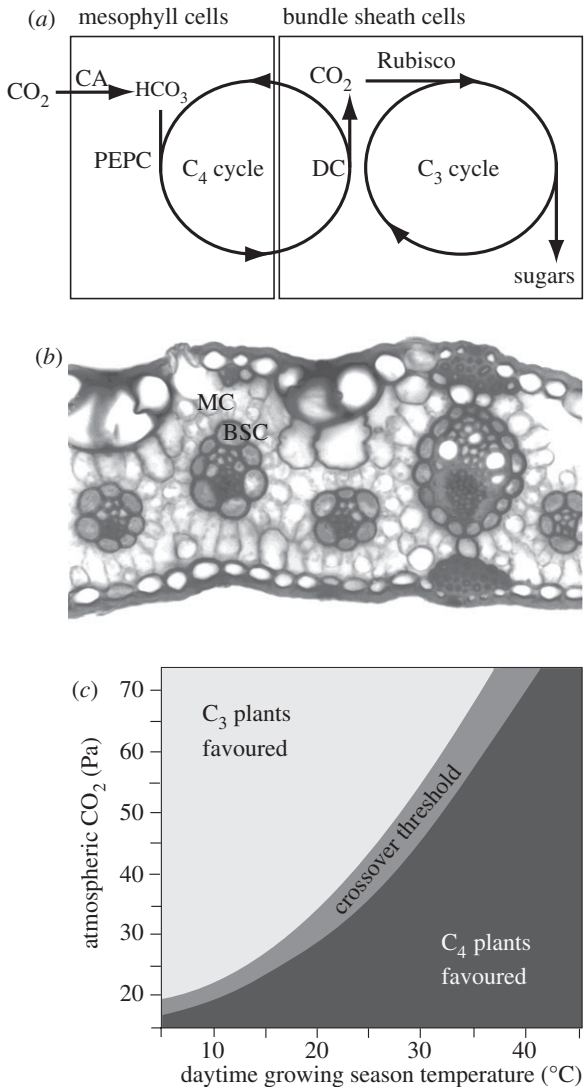

Figure 1. Mechanism of C_4 photosynthesis. (*a*) Simplified schematic of the C_4 syndrome, showing how the C_3 pathway is isolated from the atmosphere in most C_4 species within a specialized tissue composed of bundle sheath cells (BSC). The C_4 pathway captures CO_2 within mesophyll cells (MC) using the enzymes carbonic anyhdrase (CA) and phosphoenolpyruvate carboxylase (PEPC). It then transports fixed carbon to the BSC where decarboxylase enzymes (DC) liberate CO_2, which accumulates to high concentrations around Rubisco. (*b*) Transverse section of a C_4 leaf, showing the arrangement of MC and BSC. In this picture, the BSC are thicker walled, are stained darker and form rings surrounding the veins (adapted from Watson & Dallwitz [9]). Enlarged BSC relative to MC and close vein spacing are typical of C_4 leaves, and this pattern is referred to as 'Kranz anatomy'. (*c*) Explanation of how variation in CO_2 and temperature favours C_3 or C_4 species [10,11]. The schematic shows the range of CO_2 partial pressures and temperatures predicted to favour the growth of either C_3 or C_4 species, based on the maximum quantum yield of photosynthesis. Quantum yield is a measure of photosynthetic efficiency, which declines in C_3 plants as photorespiration increases at low CO_2 and high temperature, (reproduced with permission from Edwards *et al.* [3], which was adapted from Ehleringer *et al.* [11]).

evolutionary biology and geosciences has enriched our understanding of when, where and how C_4 photosynthesis evolved. Here, we extend previous work that focused on *why* the pathway evolved, based on the environmental conditions that drove natural selection. We begin by reviewing the well-established current hypothesis that atmospheric CO_2 depletion, high temperatures and open environments selected for the C_4 pathway as a means of directly improving photosynthetic rate and efficiency. Our main objective is to introduce a new dimension to these ideas, by proposing that these same environmental conditions—CO_2 depletion, high temperatures and open environments—as well as seasonal drought, would also select for C_4 photosynthesis for an additional reason; i.e. to compensate for the strain on the plant hydraulic system resulting from excessive demand for water transport. Our hypothesis is consistent with recent comparative analyses of ecological niche evolution and plant physiology, which suggest important effects of the C_4 pathway on plant–water relations. We support our proposal with evidence from the literature, and mechanistic models that integrate the latest understanding of how hydraulics, stomata and photosynthesis are coordinated within leaves. Our central focus is on grasses, but we complement our analysis with additional evidence from eudicots.

2. ENVIRONMENTAL SELECTION ON PHOTOSYNTHETIC EFFICIENCY

Atmospheric CO_2 depletion has long been advocated as the primary selection pressure for C_4 CCMs, through its differential effects on the efficiency of C_3 and C_4 photosynthesis [22]. This difference arises because the active site of Rubisco is unable to discriminate completely between CO_2 and O_2, and catalyses the fixation of both molecules [23,24]. The oxygenation reaction generates toxic intermediates that must be metabolized via photorespiration to render them harmless and to recover carbon. Oxygenation renders photosynthesis less efficient because it competes directly with carboxylation (CO_2-fixation), and because photorespiration consumes the products of photochemistry and liberates CO_2. In a C_3 plant, the ratio of carboxylation to oxygenation (and therefore photosynthetic efficiency) decreases rapidly with declining atmospheric CO_2, especially at high temperatures [25]. In contrast, by fixing the bicarbonate ion rather than CO_2, the C_4 pathway does not confuse CO_2 with O_2 (figure 1*a*). Furthermore, by isolating Rubisco from the atmosphere and concentrating CO_2 at its active site [26], it also minimizes oxygenation in the C_3 pathway. However, energy required to run the C_4 CCM imposes a cost on photosynthetic efficiency under all conditions [27,28]. This means that the efficiency of C_4 photosynthesis is only greater than the C_3 type under conditions that promote high rates of photorespiration [19]. Low atmospheric CO_2 and high temperatures are considered especially important in favouring C_4 photosynthesis, with a 'crossover threshold' for CO_2 of 35–55 Pa and temperatures of 25–30°C (figure 1*c*; [10,11]).

A further physiological difference between C_3 and C_4 species arises because the carboxylation reaction of Rubisco is strongly limited by its substrate when CO_2 falls below approximately 70 Pa at the active site [29]. Resistances to CO_2 diffusion from the atmosphere to the chloroplast mean that this limitation arises when atmospheric CO_2 levels fall below approximately 100 Pa. In contrast, significant CO_2-limitation only

occurs in C_4 plants at atmospheric CO_2 levels of less than 20 Pa [30]. The CO_2-saturation of Rubisco in C_4 photosynthesis means that in high light environments the enzyme reaches its saturated catalytic rate, maximizing the photosynthetic difference between C_3 and C_4 species. As a consequence, in open habitats, the 'crossover threshold' is raised to higher CO_2 concentrations and lower temperatures [31]. Conversely, the cool shade of forest understorey environments offers little benefit for the C_4 pathway over the C_3 type [32], although once C_4 evolves in a lineage, descendent species may invade shaded habitats by modifying their tissue costs, allowing them to maintain an advantage in photosynthetic rate over co-occurring C_3 species [33].

Water relations have previously been proposed to influence the evolution of C_4 photosynthesis in an indirect way. For terrestrial vascular plants, the loss of water is an inevitable cost of photosynthesis, regulated by turgor-mediated decreases in the aperture of stomatal pores. The partial closure of stomata to conserve water in arid and saline soils or dry atmospheric conditions (characterized by high vapour pressure deficit (VPD)) has been hypothesized to select for the C_4 pathway via indirect effects on photosynthetic efficiency [34]. Thus, reduced stomatal aperture (i) restricts the CO_2 supply to photosynthesis and (ii) decreases transpiration, thereby reducing latent heat loss and raising leaf temperature. Both effects increase photorespiration, depressing the efficiency of C_3 photosynthesis, and favouring the C_4 type.

Therefore, the general expectation based on physiological evidence is that declining atmospheric CO_2 should select for C_4 photosynthesis in hot, open and dry or saline environments, where photorespiration is especially high in C_3 species [19].

3. ECOLOGICAL DRIVERS OF C_4 PATHWAY EVOLUTION

Recent data on the timing of C_4 origins and geological history have supported these ideas for the importance of low CO_2 and high temperature and irradiance, but also highlight the importance of aridity. First, the modelling of evolutionary transitions from C_3 to C_4 photosynthesis using time-calibrated molecular phylogenies indicated that C_4 origins have all occurred over the past 30 Myr, with no difference in timing between monocot and eudicot lineages (figure 2) [35–37]. Secondly, multiple geological proxies suggested that atmospheric CO_2 has remained below 60 Pa for most of this 30 Myr interval (figure 2), after a dramatic decline during the Oligocene (23–34 Ma) that corresponds to the onset of Antarctic glaciation [4]. Therefore, C_4 photosynthesis does seem to have evolved in a CO_2-depleted atmosphere, within the ranges of uncertainty that are inherent to phylogenetic and geological evidence [4,37].

The hypothesis that high temperatures select for C_4 photosynthesis has been supported for 30 years by invoking the observation that species richness of C_4 grasses increases along latitudinal and altitudinal temperature gradients [32,38,39]. However, phylogenetic comparative analyses have shown that C_4 species do not live in warmer environments than their closest C_3 relatives. First, Edwards & Still [40] showed that the absence of C_4 species from high altitudes in the predominantly exotic grass flora of Hawaii [39] is better explained by phylogenetic history than photosynthetic pathway. The exclusively C_3 lineage Pooideae is most speciose at cool, high elevations. However, species of the PACMAD lineage are most numerous in the warm lowlands, irrespective of whether they use C_3 or C_4 photosynthesis. Edwards & Smith [41] further investigated this pattern by reconstructing the evolution of temperature niche in the world's grasses. Their analysis indicated that grasses originated in the tropics. The C_3 and C_4 species of the PACMAD clade have remained predominantly in these warm environments, irrespective of photosynthetic pathway, while Pooideae have adapted to and radiated in low-temperature environments. Thus, C_4 photosynthesis did evolve at high temperatures, but the major innovation that caused ecological sorting of grasses along temperature gradients was the adaptation of certain C_3 lineages to cold conditions [41].

Comparative analyses also support the hypothesis that the C_4 pathway in grasses evolved in open environments. First, by modelling the rate of evolutionary transitions between C_3 and C_4 photosynthesis, and shaded and open habitats, Osborne & Freckleton [42] showed that C_4 origins were significantly more likely to have occurred in open than shaded environments. Secondly, Edwards & Smith [41] quantified the shift in environmental niche that is correlated with evolutionary transitions from C_3 to C_4 photosynthesis.

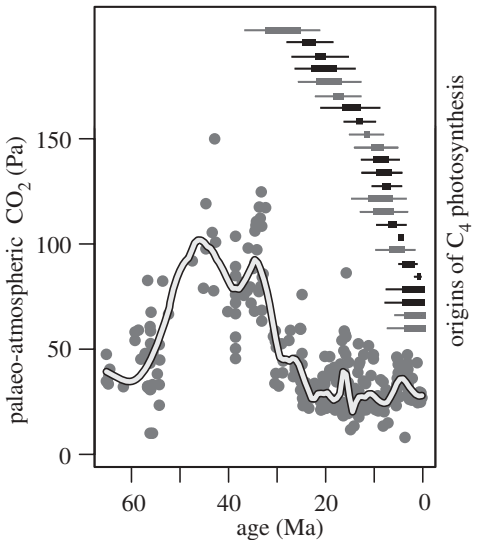

Figure 2. Geological history of atmospheric CO_2 and the estimated ages of C_4 evolutionary origins. The palaeo-atmospheric CO_2 history of the Cenozoic is reconstructed from multiple independent proxies (pale grey circles), with a smoothed line of best fit encompassing all of the evidence (reproduced with permission from Beerling & Royer [4]). The estimated ages of C_4 evolutionary origins in grasses (dark grey horizontal bars) and eudicots (black horizontal bars) were obtained using phylogenetic inference and calibration to fossils [35]. Thick bars represent uncertainty in the position of each C_4 evolutionary origin on the phylogeny, while thin bars indicate uncertainty in dating of the phylogeny (reproduced with permission from Christin *et al.* [35]).

The origins of C_4 photosynthesis were generally associated with migration from an aseasonal tropical niche into a seasonal, sub-tropical one, an ecological shift consistent with a transition from moist tropical forest to drier, more open woodland or savannah habitats [41]. These complementary analyses suggest that C_4 photosynthesis evolved in C_3 species that had migrated out of their ancestral niche in tropical forests, and invaded open sub-tropical woodland or savannah habitats. The C_4 pathway, therefore, seems to be a key adaptation to one of the most important ecological transitions in the evolutionary history of grasses [43], which ultimately enabled the assembly of the tropical grassland biome.

The proportion of C_4 species in eudicot floras increases along gradients of rising aridity [11]. Recent comparative analyses at the regional and global scales show that, in addition to preferring open habitats, C_4 grasses have also sorted into drier environmental niches than their C_3 relatives [40–42]. However, for grasses, there is no evidence that C_4 photosynthesis is more likely to evolve in xeric than mesic habitats [42]. Rather, the distribution of C_4 species in dry areas can be explained by two inferences from comparative analyses: (i) that C_4 origins were accompanied by shifts to a drier ecological niche within the humid sub-tropics [41] and (ii) a greater likelihood that C_4 than C_3 lineages will invade very dry (xeric) environments [42]. In some systems, C_4 grasses tolerate greater aridity than C_3 species of adjacent areas; for example, it has been argued that certain C_4 grasses of the Kalahari occur in areas too dry for the C_3 type to persist [44]. Water relations clearly play an important role in the ecology and biogeography of both C_4 monocots and C_4 eudicots.

A corpus of physiological work and comparative analyses therefore supports the theory of how low atmospheric CO_2 drove selection for improved photosynthetic rate and efficiency in hot and open environments over the last 30 Myr. What has been missing is an understanding of the importance of plant–water relations in differentiating photosynthetic types in such environments.

4. STRAIN ON PLANT–WATER RELATIONS IN A CO_2-DEPLETED ATMOSPHERE

Multiple strands of geological, ecological and physiological evidence indicate that a restriction in water supply and an increase in evaporative demand were important ecological factors during the evolution of C_4 species. First, permanent ice sheets of low CO_2 'icehouse' climate intervals are known to reduce atmospheric moisture levels, with cool temperatures reducing the intensity of the hydrological cycle and increasing climatic seasonality [45]. As a consequence, the CO_2-depleted 'icehouse' climate of the last 30 Myr has caused the ecological availability of water to decline across large parts of the Earth's surface.

Paleontological evidence reveals that open woodland, savannah and grassland vegetation had begun to extend over large areas of the tropics and subtropics by the Miocene (24–6 Ma) [3,46]. By analogy with processes in the modern world, these open tropical and sub-tropical ecosystems are likely to have been generated by seasonal aridity, edaphic conditions that exclude trees (including high salinity), and disturbance by fire and large mammalian herbivores [3,47–49]. Low atmospheric CO_2 may interact with each of these processes by limiting tree growth [50–52]. In fire-prone environments, this limitation means that trees are less likely to become large enough to survive surface fires [51,53]. Indeed, in contemporary mesic savannahs, woody plant cover is apparently increasing in response to rising CO_2 [53]. C_4 plants are generally short-statured herbs, and only trees in exceptionally rare cases (several species of Hawaiian C_4 *Euphorbia* are fully trees, including rainforest as well as dry forest species; and *Haloxylon* trees of West Asia have C_4 photosynthetic stems). The central role of seasonal aridity in reducing forest cover therefore means that the early C_4 plants living in open tropical and sub-tropical environments may well have been subjected to fire events and/or episodes of soil drying.

The demand for water imposed by potential evapotranspiration (PET) is also significantly greater for plants in open habitats than in shaded understorey environments. This environmental contrast is caused by a suite of interrelated microclimatic effects associated with tree cover, illustrated in figure 3 using field observations and a model of leaf energy balance and evaporation (appendix A). Micrometeorological data are shown in figure 3*a*,*b* for transects crossing a rainforest edge into adjacent pasture in tropical (Mexico) and temperate (New Zealand) localities [54,55]. Closed forest canopies typically intercept greater than 95 per cent of incident shortwave radiation (figure 3*a*,*b*). A model of leaf energy balance shows that this markedly reduces the net radiation and therefore the energy available to drive evaporation (latent heat flux) at ground level (figure 3*c*,*d*). Shading of the land surface under a forest canopy also causes a decrease in the air temperature at ground level (from 28 to 25°C in the tropical example, and from 10 to 5°C in the temperate example; figure 3). Therefore, the vapour pressure gradient driving transpiration, as indicated by the VPD, also declines (figure 3*a*,*b*). Finally, windspeed is lower in forested compared with open environments (figure 3*a*,*b*). This reduces the leaf boundary layer conductance to water vapour (figure 3*e*,*f*) and further slows the modelled rate of evaporation. The overall effect of this micrometeorological gradient is a massive difference in the PET modelled for leaves in forested compared with open environments (figure 3*e*,*f*; appendix A). In the examples illustrated in figure 3, modelled PET is close to zero in the humid forest understorey, but exceeds 10 mmol $H_2O\ m^{-2}\ s^{-1}$ in the adjacent open pasture for both tropical and temperate climates (figure 3*e*,*f*).

In fact, the risk of colonizing exposed habits depends on the actual rate of leaf transpiration (E), which is lower than PET, being determined by the coupling of micrometeorological effects with the leaf stomatal conductance to water vapour (g_s). The g_s is controlled by changes in stomatal aperture, which are regulated by leaf water status, photosynthetic rate and chemical signals reflecting the soil water status transmitted from roots to leaves [56]. The g_s plays a pivotal role in leaf

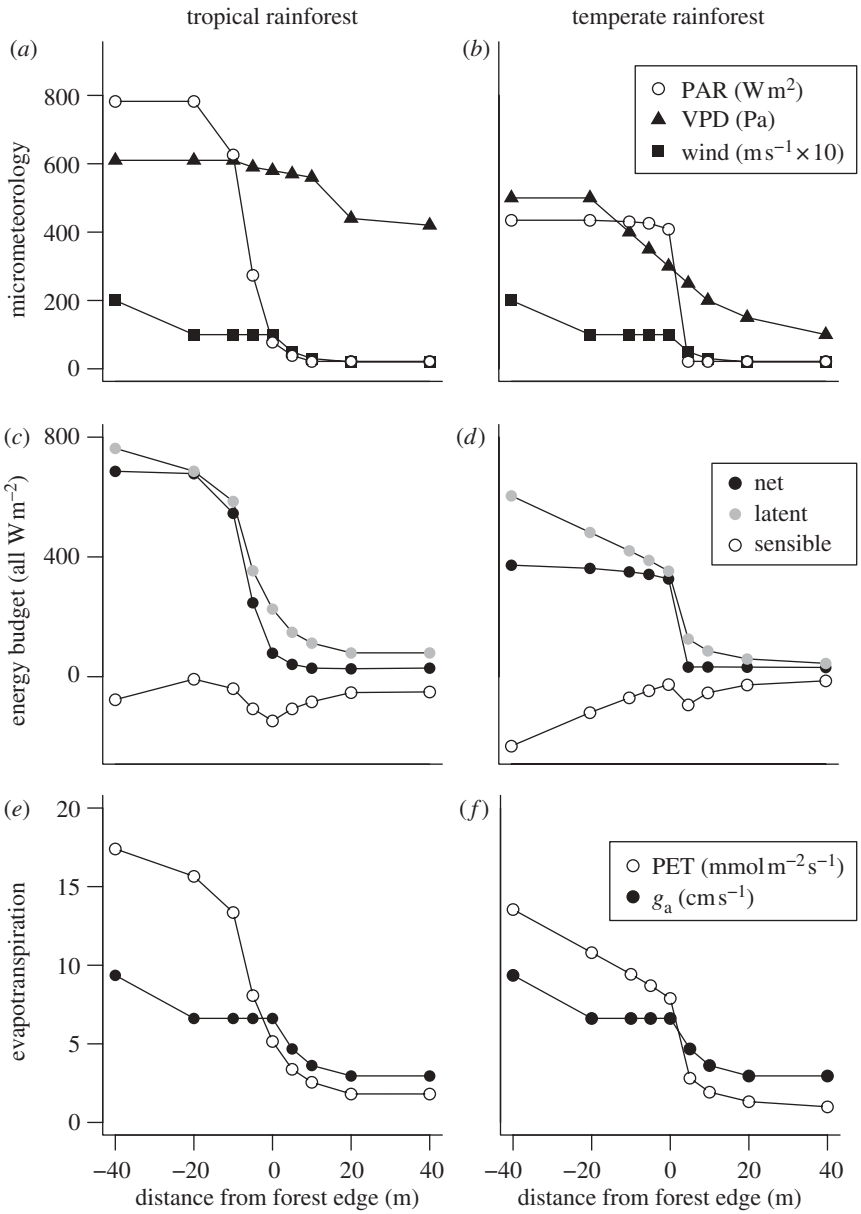

Figure 3. Micrometeorological gradient spanning the transition from forested to open habitats. Data are shown for (*a*,*c*,*e*) pasture at the edge of tropical rainforest and (*b*,*d*,*f*) temperate rainforest, plotted against distance into the forest (negative values for distance = pasture; positive values = forest). Micrometeorological observations of photosynthetically active radiation (PAR), vapour pressure deficit (VPD) and surface windspeed are shown for (*a*) Mexico [54] and (*b*) New Zealand [55]. From these data, net radiation, latent and sensible heat fluxes are calculated using the model outlined in appendix A for the (*c*) tropical and (*d*) temperate forests. Calculated values of potential evapotranspiration (PET) and boundary layer conductance (g_a) are also shown for the same (*e*) tropical and (*f*) temperate localities.

gas exchange, limiting both the efflux of water and influx of CO_2, and the C_4 CCM causes a large shift in this trade-off between carbon gain and water loss. For any given value of g_s, the net rate of leaf photosynthetic CO_2 uptake (A) is greater for C_4 than C_3 species. This contrast is illustrated in figure 4*a* for interspecific comparisons of closely related C_3 and C_4 PACMAD grass species. Measurements were made under modern atmospheric CO_2 levels, and in high light and temperature conditions representative of a warm, open environment. The contrast is also modelled in figure 4*b* using models of leaf gas exchange for idealized C_3 [59] and C_4 [29] species (see appendix B). In the interspecific comparison, photosynthesis at 30°C can span the same range in C_3 and C_4 species, with one exceptionally high value of A in the C_3 species exceeding the highest values observed in the C_4 species (figure 4*a*; [57]). However, high A for C_3 species comes at enormous cost in terms of g_s (figure 4*a*,*b*), and elevated rates of CO_2-fixation are therefore achieved with far greater water economy in C_4 than C_3 leaves (i.e. with greater water-use efficiency (WUE), defined as A relative to E). The ecological significance of this difference is underscored by the fact that the exceptionally high C_3 value of A in figure 4*a* was measured in the wetland species *Phragmites australis*, whereas the highest C_4 value was in the savannah species *Eriachne aristidea* [57].

The greater WUE of C_4 compared with C_3 photosynthesis arises from both differences in stomatal

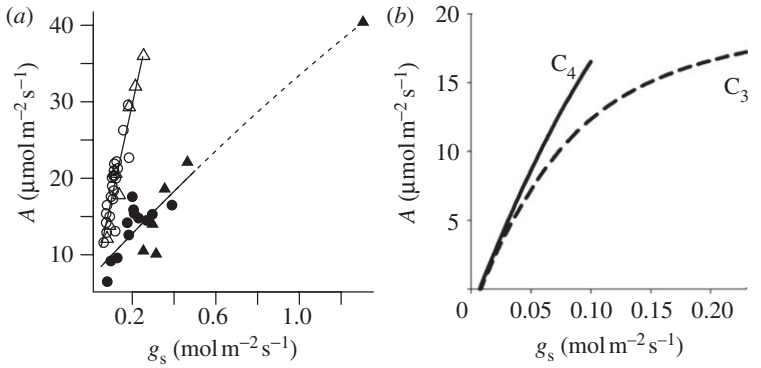

Figure 4. Illustration of the relationships of photosynthesis (A) to stomatal conductance (g_s) in C_3 and C_4 species [57,58]. (*a*) Interspecific comparison of PACMAD grass species under high light and the current ambient CO_2 level (filled symbols, C_3; open symbols, C_4; circles from Taylor *et al.* [58], photosynthetic photon flux density (PPFD) = 1300 μmol m^{-2} s^{-1}, temperature = approx. 25°C, VPD = 1 kPa; triangles from Taylor *et al.* [57], PPFD = 2500 μmol m^{-2} s^{-1}, temperature = 30°C, VPD = 0.8–1.5 kPa). Fitting a general linear model to these data showed that the slope of A on g_s was significantly steeper among C_4 than C_3 species (125 versus 29 μmol CO_2 mol^{-1} H_2O, respectively; $F_{1,42} = 55.8$, $p < 0.0001$), with a significant quadratic term that shows no interaction with photosynthetic pathway. (*b*) Intraspecific response simulated for a C_3 and a C_4 species by prescribing variation in g_s, and modelling A using the approach described in appendix B. Note the saturation response in C_3 and linear response in C_4, indicating the greater sensitivity of A to stomatal closure in C_4, despite achieving higher maximum A at its maximum g_s.

aperture and the kinetic properties of the carboxylase enzymes employed by each pathway (figure 1*a*). PEPC in C_4 plants is able to fix carbon at a much higher rate than Rubisco in C_3 plants at *in vivo* substrate concentrations [29]. This allows the C_4 pathway to generate a much steeper air–leaf CO_2 gradient and higher rates of photosynthesis for a given value of g_s. The lower E and greater WUE of C_4 than C_3 plants was first recognized more than 40 years ago [60], although it is subject to ecological adaptation that can lead to significant interspecific variation and thus overlaps in the ranges of photosynthesis and transpiration for the two photosynthetic types [61]. However, recent work sampling multiple independent lineages of C_4 grasses from a range of different habitats showed that g_s is significantly lower in each lineage of C_4 species than in closely related lineages of C_3 grasses [57,58].

The need for a lower g_s to conserve water is especially strong when CO_2 levels fall and leaves tend to open stomata to maintain photosynthesis. Data compiled from five independent experiments demonstrate that g_s in both C_3 and C_4 plants increases dramatically in response to the depletion of atmospheric CO_2 to sub-ambient levels (figure 5). This negative relationship of g_s to CO_2 is apparently independent of the responsiveness of g_s to VPD [68], and partially or fully offsets the CO_2-limitation of photosynthesis at the cost of greater water use. A general linear model fitted to ln-transformed data shows a significant effect of photosynthetic pathway on the intercept of this relationship of g_s to CO_2 depletion, supporting the generality of higher g_s in C_3 than C_4 species (figure 5*a*). However, there is no difference in the slope of this relationship between C_3 and C_4 species (figure 5), indicating a similar relative increase in g_s with declining atmospheric CO_2 for C_3 and C_4 species. This finding is consistent with previous meta-analyses showing similar relative declines in g_s with CO_2 enrichment in C_3 and C_4 grasses [66,67]. Notably, because g_s is typically higher in C_3 than C_4 species, a similar relative response to CO_2 translates into a larger absolute effect (figure 5*b*). For example, for the model fitted in figure 5*b*, a depletion of atmospheric CO_2 from 100 to 30 Pa equivalent to the Oligocene CO_2 drop (figure 2) results in a rise in g_s from 0.23 to 0.61 mol H_2O m^{-2} s^{-1} in C_3, but only from 0.08 to 0.21 mol H_2O m^{-2} s^{-1} in C_4 species.

We explored the implications of these contrasting stomatal responses to CO_2 in C_3 and C_4 leaves by modelling leaf transpiration and energy balance (appendix A). Simulations with the model made the simplifying assumption that stomata respond only directly to CO_2, with no hydraulic or hormonal feedback on g_s. We compared the modelled response of E to CO_2 under four sets of micrometeorological conditions representing either an open pasture or a shaded rainforest understorey, in a humid tropical or temperate climate (using the data from figure 3). Our model simulations showed that falling atmospheric CO_2 drove larger increases of g_s and E in C_3 than C_4 species (figure 6*a*,*b*); this contrast was especially pronounced in open, tropical environments (figure 6*a*). For the simulations shown in figure 6*a*, we used a high relative humidity of 80 per cent (VPD = 0.6 kPa), which is typical of the moist tropics and the summer growing season in the humid subtropics (e.g. figure 3*a*). Under these conditions, simulated E in the C_3 species exceeded 6 mmol H_2O m^{-2} s^{-1} Mpa^{-1} at a CO_2 level of less than 40 Pa (figure 6*a*). Assuming a leaf-specific whole- plant hydraulic conductance (K_{plant}) of 12 mmol H_2O m^{-2} s^{-1} in grasses, and a 50 per cent decline in K_{plant} under a soil–leaf water potential gradient of −1 MPa [69], this transpiration rate would be sufficient to cause 50 per cent failure of the hydraulic system. The threshold was not reached in a C_4 leaf under these conditions. In a drier atmosphere of 60 per cent relative humidity (VPD = 1.5 kPa), the threshold for 50 per cent hydraulic failure in the C_3 leaf was reached at $CO_2 < 80$ Pa, and in the C_4 at < 20 Pa (data not shown). The contrast was yet more pronounced at a VPD of 3.0 kPa, which is typical of hot, arid climates. Here, 50 per cent hydraulic failure

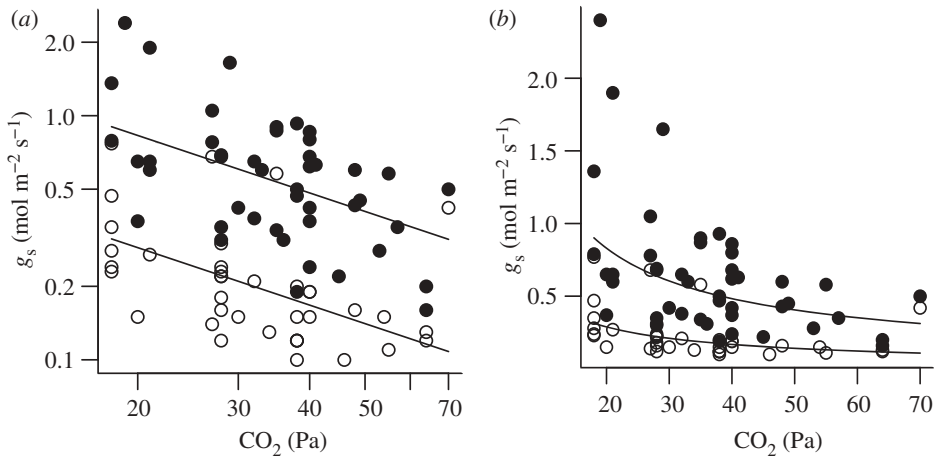

Figure 5. Stomatal conductance (g_s) for the leaves of C_3 and C_4 plants grown and measured under a range of different CO_2 partial pressures, with an emphasis on experiments investigating the effects of CO_2 below the current ambient level of approximately 40 Pa (data sources: [30,62–65]; electronic supplementary material). The data compilation is based on literature searches for studies reporting the leaf gas exchange of plants under sub-ambient CO_2. However, values for elevated CO_2 were included when they were reported as part of the same CO_2-gradient studies. The fitted curve for the C_3 species is $\ln(g_s) = 2.16 - 0.78 \ln(CO_2)$, and for the C_4 is $\ln(g_s) = 1.10 - 0.78 \ln(CO_2)$. Data and curves are shown on (*a*) log and (*b*) linear plots to illustrate relative and absolute sensitivity to CO_2, respectively. The fitted curves produce effect sizes for g_s at elevated CO_2 in C_3 and C_4 grasses that fall within confidence intervals of previous meta-analyses [66,67]. Filled circles, C_3; open circles, C_4.

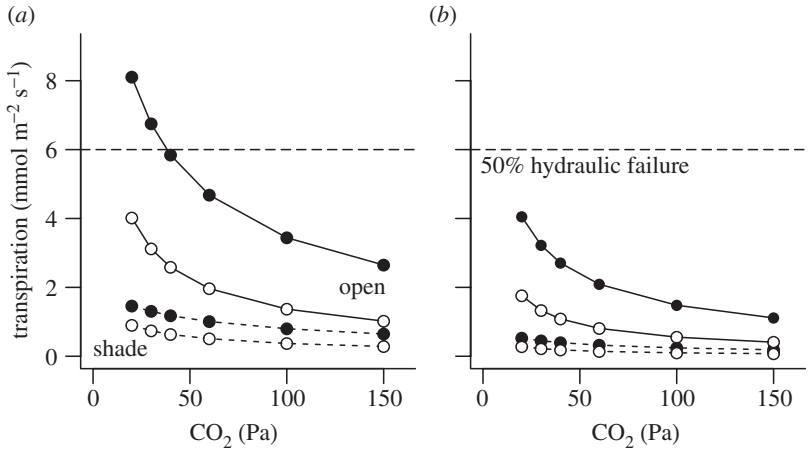

Figure 6. Modelled response of transpiration to CO_2 for C_3 and C_4 leaves in open (solid lines) and shaded rainforest understorey (dashed lines) conditions in either (*a*) humid tropical or (*b*) humid temperate climates. The model is described in appendix A. Horizontal dashed lines indicate the transpiration rate that would cause 50% hydraulic failure in the absence of feedbacks on stomatal conductance. Filled circles, C_3; open circles, C_4.

occurred for the C_3 leaf at $CO_2 < 150$ Pa, and for the C_4 leaf at $CO_2 < 50$ Pa (data not shown).

Thus, to avoid failure of the vascular system in open, tropical environments, hydraulic regulation of stomata, investment in hydraulic supply, or a reduction in leaf area [62], would be required at a considerably higher atmospheric CO_2 partial pressure in C_3 than C_4 species. Coupled with the inference that open tropical habitats selected for the C_4 pathway in grasses, this observation points strongly to plant–water relations as a potential driver of C_4 evolution.

5. HYPOTHESIS FOR A CENTRAL IMPORTANCE OF HYDRAULICS IN C_4 EVOLUTION

The current consensus model for the evolution of C_4 photosynthesis has been developed over 25 years [19]. The evolutionary trajectory from C_3 to C_4 photosynthesis, via C_3–C_4 intermediates, is framed in terms of distinct phases for the sake of clarity; however, in reality, these are likely to overlap, and certain developments may occur earlier or later in the sequence. A simplified model of the phases is outlined in table 1, and Sage [19] provides both a comprehensive review of the evidence underpinning this model and the detailed mechanisms proposed. As with the evolution of any complex trait, each step must provide a selective advantage over the previous phase or be selectively neutral.

We propose that atmospheric CO_2 depletion and open environments select indirectly for C_4 photosynthesis via plant–water relations at two points during the evolutionary sequence (table 1, phases 1 and 3). This mechanism acts in combination with

Table 1. Hypothetical model for the evolution of C_4 photosynthesis, showing three phases that are each observed in extant C_3–C_4 intermediates. The scheme is a simplified version of that presented by Sage [19], incorporating new evidence [70].

phase 1. Evolution of 'proto-Kranz anatomy'

A reduction in the distance between leaf veins and an enlargement in bundle sheath cells (BSC) (figure 1*b*) may evolve under dry environmental conditions to enhance leaf water status [19,71,72]. Since photosynthetic activity is limited in the BSC of most C_3 leaves, increases in the number of chloroplasts may initially serve to maintain leaf light absorpance as the BSC occupy a larger fraction of the leaf. An increase in the numbers and asymmetric distribution of mitochondria in the BSC may establish a photorespiratory CO_2 pump that shuttles glycine and refixes CO_2 *within* single BSC (see phase 2). This combination of traits has been termed 'proto-Kranz anatomy', and occurs in C_3 species that are closely related to C_3–C_4 intermediates [70].

phase 2. Evolution of a photorespiratory CO_2 pump

Photorespiration liberates CO_2 via a decarboxylation reaction catalysed by the enzyme glycine decarboxylase (GDC). The increasing localization of this enzyme in BSC mitochondria requires glycine to be shuttled *between* the mesophyll cells (MC) and the BSC, liberating CO_2 in the BSC and allowing its refixation by Rubisco in this compartment (figure 1*b*). Efficiency of the glycine shuttle increases greatly if BSC walls are resistant to CO_2 diffusion, thereby concentrating CO_2 in the BSC. This type of photorespiratory CO_2 pump is typical of C_3–C_4 intermediates [19].

phase 3. Evolution of the C_4 cycle

Increases in the PEPC activity of MC may occur initially to scavenge CO_2 that leaks from the BSC, but eventually allows the fixation of CO_2 from intercellular airspaces (figure 1*a*). Once this occurs, enhancement of decarboxylase enzyme activities in the BSC is needed to recover the acceptor molecule for carbon-fixation (figure 1*a*). As carbon-fixation by PEPC increases above that of Rubisco, the C_3 cycle is increasingly confined to the BSC, and activities of the C_4 and C_3 cycles are coordinated. Finally, enzymes recruited into the C_4 cycle adapt to their new catalytic environment via changes in turnover rate, substrate affinity and regulation. Changes in stomatal conductance occur during this phase [19].

the well-established effects of atmospheric CO_2 depletion and open environments on photorespiration. A direct role of water relations provides a clear explanation for many of the anatomical changes in the early evolution of C_3–C_4 intermediacy; these are observed in other lineages of C_3, C_4 and CAM species, which indicates that these steps are not rare or extraordinary events, but that C_4 evolution simply co-opts typical steps in adaptation to dry environments.

Evolution of 'proto-Kranz anatomy' (table 1, phase 1). Our hypothesized hydraulic mechanism is based on the vulnerability of C_3 leaves to desiccation and hydraulic failure under conditions of high evaporative demand in hot, open environments. Indeed, as described above, the hydraulic vulnerability of leaves would have increased dramatically as C_3 grass species migrated from the understorey of a tropical forest into more open tropical environments. If stomata close to protect the hydraulic system, the plant eventually faces carbon starvation through photorespiration and the depletion of carbon stores [73,74]. Carbon starvation is also exacerbated by atmospheric CO_2 depletion [75]. These conditions would select for greater hydraulic capacity in C_3 leaves, enabling greater g_s to achieve rapid rates of photosynthesis in periods when water is abundant, and reducing both the requirement for stomatal closure and the risk of hydraulic failure as stomata partially close in a drying soil or under increasing VPD.

Notably, the anatomical preconditioning required for C_4 is precisely that expected to evolve in C_3 plants under selection for greater tolerance of dry soil, open environments, high VPD and/or low CO_2. Previous studies of adaptation to these conditions within species or across closely related species within given lineages have shown increased vein densities, and thus shorter interveinal distances [76–79]. This higher vein density would permit greater g_s and higher A during periods with high water availability, to compensate for low CO_2. Indeed, the evolution of greater vein density in the early angiosperms may have allowed them to better cope with low CO_2, while avoiding stomatal closure, contributing to or driving their contemporary dominance of world vegetation [78,80]. The higher vein densities in C_4 than C_3 species may indicate an extension of that trend, i.e. an adaptation to the water deficit that accompanies higher demand from transpiration to maintain photosynthetic rate in low CO_2. In the same way that an increase in vein density may have enabled angiosperms to displace gymnosperms in dominating the world's forests, this trend in grasses may have provided a competitive advantage over grasses with lower vein densities, contributing to their dominance over large areas of the planet. The high vein densities in species with 'proto-Kranz anatomy' led to this feature being co-opted as an early part of the C_4 syndrome, providing enough tissue to later serve as the locus of sequestered C_3 metabolism (figure 1*a*,*b*) [19,71,72,81,82].

Similarly, the enlargement of bundle sheath during the early phase of C_4 evolution may have contributed water storage capacitance to the tissue [19,71]. Indeed, the evolution of such tissue in species with 'proto-Kranz anatomy' would be an extension of a frequently observed trend in certain plant lineages in which the species adapted to saline and drier climates have more strongly developed achlorophyllous, large-celled tissue. This tissue serves an apparent function for water storage either in the bundle sheath, mesophyll or hypodermal layers, and this trend of greater water storage with aridity is apparent within C_3 lineages with leaves [83,84] and phyllodes [85], but also within C_4 and CAM lineages [86,87] (M. J. Sporck & L. Sack 2011, unpublished data).

Evolution of the C_4 cycle (table 1, phase 3). The evolution of greater WUE is apparently an important step in C_4 evolution. It may be achieved in certain C_3–C_4 intermediates operating a photorespiratory pump (table 1, phase 2) through the enhancement of A for a

given g_s (e.g. *Heliotropium* [88]). However, once the carboxylase activity of PEPC exceeds that of Rubisco (evolution of 'C_4-like' plants during phase 3, table 1), further improvements in WUE may occur through reduced g_s (e.g. *Flaveria* [89]). Thus, evolution towards C_4 probably first involved a suppression of photorespiration (table 1, phase 2) and then increased PEPC activity (table 1, phase 3), but only this last step enabled a reduction of g_s. These steps may even occur within C_3 species: populations of the grass *Phragmites australis* in hot, arid and saline environments show increasing investment in elements required for the C_4 cycle, including PEPC, decarboxylase enzymes and bundle sheath tissues, which may enhance both CO_2-fixation and WUE [90]. Thus, the engagement of CO_2-fixation via PEPC (table 1, phase 3) improves leaf–water relations, allowing a lower value of g_s for a given rate of photosynthesis, and thus a smaller absolute response of g_s to CO_2 depletion in C_4 leaves (figure 5*b*). This benefit would lead atmospheric CO_2 depletion and open environments to select for the C_4 cycle via plant–water relations, as well as via their effects on photosynthetic efficiency. Together, these physiological differences mean that leaves operating a fully integrated C_4 cycle are less prone than C_3 leaves to hydraulic failure or stomatal closure in hot, open environments. This contrast in sensitivity to water deficit increases dramatically under atmospheric CO_2 depletion.

A greater hydraulic conductance relative to demand, as would arise from the adaptation described, would result in a greater ability to maintain open stomata during soil drying events in C_4 than C_3 leaves, and a lower sensitivity of stomata to increases in VPD and to decreases in CO_2 (see §6). These improvements in water relations provide a plausible physiological basis for the greater likelihood for C_4 than C_3 grass lineages to invade xeric environments [42].

6. HYDRAULIC FEEDBACKS ON LEAF PHYSIOLOGY

Our hypothesis that C_4 evolved not only to improve photosynthetic efficiency *per se*, but also to reduce water stress by enabling low g_s, has additional implications that at first sight lead to inconsistency. While the C_4 species can achieve higher A for a given g_s, A declines more rapidly as g_s decreases (figure 4*a*,*b*). Because of this greater sensitivity of A to g_s, a C_4 plant must keep stomata open to maintain its advantage in A over C_3 plants. At first sight, this problem should render photosynthesis in C_4 plants particularly sensitive to soil drying owing to stomatal closure. As an initial test of our hypothesis for a hydraulics-mediated advantage of C_4 photosynthesis, and to further explore the physiological implications, we used a novel integrated model of leaf photosynthesis, stomatal and hydraulic systems to compare the physiological behaviour of C_3 and C_4 species (appendix B), with a particular focus on conditions of CO_2 depletion (low CO_2), atmospheric water vapour deficit (high VPD) and soil drying (low soil water potential). Given reasonable assumptions, these model simulations supported the hypothesis of a hydraulically based advantage of the C_4 syndrome under high VPD and low soil water potential, enabling stomata to remain open, and maintaining A at higher levels than C_3 species, with greatest differences at low CO_2.

We tested the role of hydraulic conductance in allowing g_s and A to be maintained during drought under varying VPD and atmospheric CO_2 in C_3 and C_4 species. We parametrized the model using data from the literature, and coupled this with photosynthesis models for C_3 and C_4 types (appendix B). Thus, we compared C_3 and C_4 species that differed in g_s (0.23 versus 0.10 mol m^{-2} s^{-1}, respectively) but assumed the same responsiveness of g_s, and the same vulnerability of the hydraulic system, to declining leaf water potential. We tested three scenarios, with the C_4 species having: the same whole-plant hydraulic conductance (K_{plant}) as the C_3 species; double the K_{plant}; or half the K_{plant} (figures 7 and 8).

When the C_4 species had the same K_{plant} as the C_3, the C_4 was able to maintain g_s at a higher relative level (percentage of its maximum value) as the soil dried; this advantage over the C_3 was especially strong at higher VPD (figure 7). This result is consistent with an experimental comparison of PACMAD grasses under drought, which showed a more sensitive response of g_s to soil water deficits in C_3 species than in closely related C_4 species [57]. Model simulations also showed lower leaf water potential in the C_3 than C_4 species as soil dried, until the point of stomatal closure, where the leaves equilibrated with the soil (figure 7). This contrast is also broadly consistent with comparative experiments on closely related C_3 and C_4 PACMAD grasses, which showed a difference in leaf water potential under moist conditions that was diminished under chronic drought [57,68]. In our model simulations, this advantage was evidently owing to the higher K_{plant} relative to g_s for the C_4 over C_3 species. When the C_4 plant was given double the K_{plant} of the C_3 species, its advantage in maintaining open stomata during soil and atmospheric drought was increased, and when the C_4 plant was given half the K_{plant} of the C_3 species, its advantage was diminished.

The ability of a C_4 species with similar or higher K_{plant} to a C_3 species to maintain open stomata during drought also translated into an ability to maintain A at a higher level. This advantage went beyond compensating for the tendency of A to decline more precipitously with declining g_s in C_4 than C_3 species, described above (figure 4*a*,*b*), and typically provided C_4 species with an ability to maintain higher A during mild drought, especially at higher VPD (notably, simulations at yet higher VPDs led to even stronger differences between photosynthetic types). When the C_3 and C_4 species had the same K_{plant}, A was higher in the C_4 than the C_3 under low CO_2, but the rank was reversed under high CO_2 (figure 8). Doubling the value of K_{plant} in C_4 compared with C_3 species gave an advantage in A, and the ability to maintain photosynthesis during drought. This finding is broadly consistent with an early demonstration that, during the dry season in the Negev desert, the C_4 species *Hammada scoparia* showed a shallower decline of A with declining leaf water potential than three C_3 species (*Prunus armeniaca*, *Artemisia herba-alba* and *Zygophyllum dumosum*). At a leaf water potential of −6 MPa, *H. scoparia* (C_4) had twice the A of these C_3

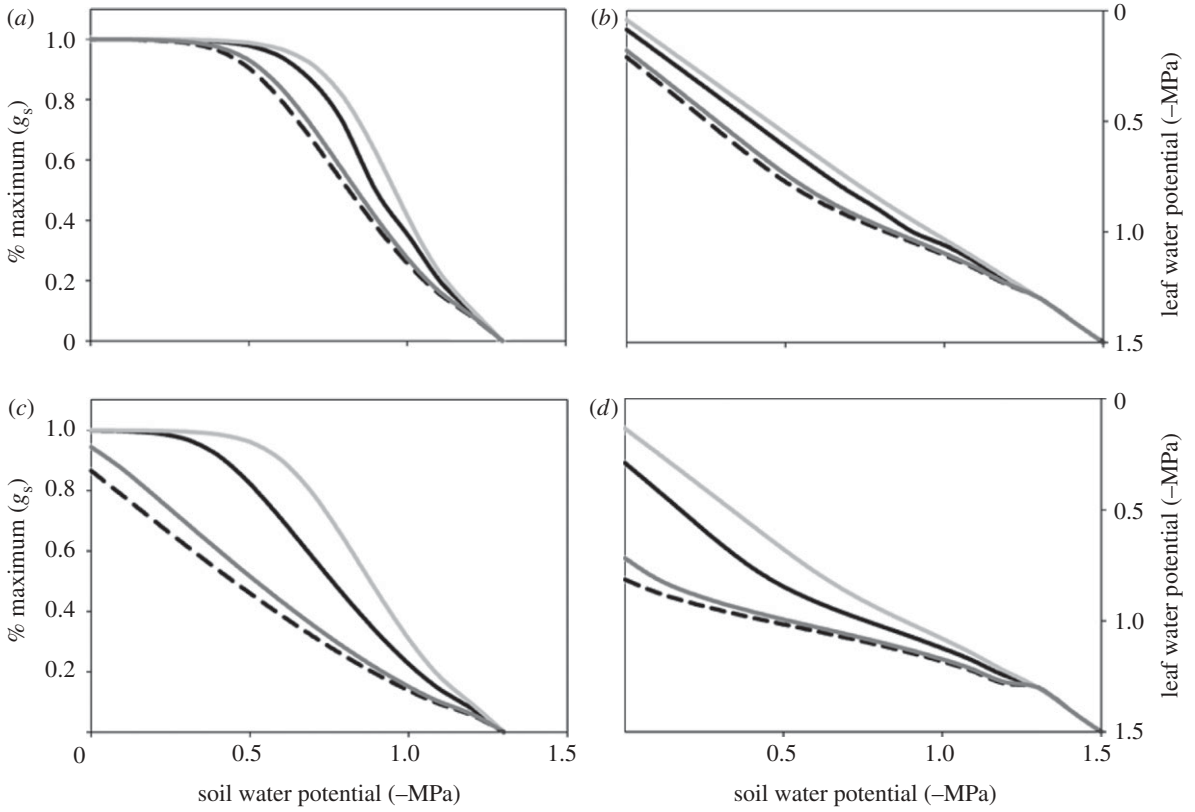

Figure 7. Simulated response of mid-day operating stomatal conductance (as a percentage of maximum for hydrated leaves) and leaf water potential to drying soil at VPD of (*a*,*b*) 1 kPa and (*c*,*d*) 3 kPa, for a C_3 species and C_4 species with identical plant hydraulic conductance (K_{plant}), for a simulated C_4 species with double the K_{plant}, and for a simulated C_4 species with half the K_{plant} (corresponding to its value of g_s being approximately half that of the C_3 species). Note that the C_4 species maintains stomatal opening into drier soil and higher VPD than the C_3. Increasing the K_{plant} improves this ability in the C_4 species, whereas reducing the K_{plant} by half leads to very rapid decline of g_s at high VPD or in a dry soil. (*a*–*d*) Dashed line, C_3; black solid line, C_4; light grey solid line, C_4, $2 \times K_{plant}$; dark grey solid line, C_4, $0.5 \times K_{plant}$.

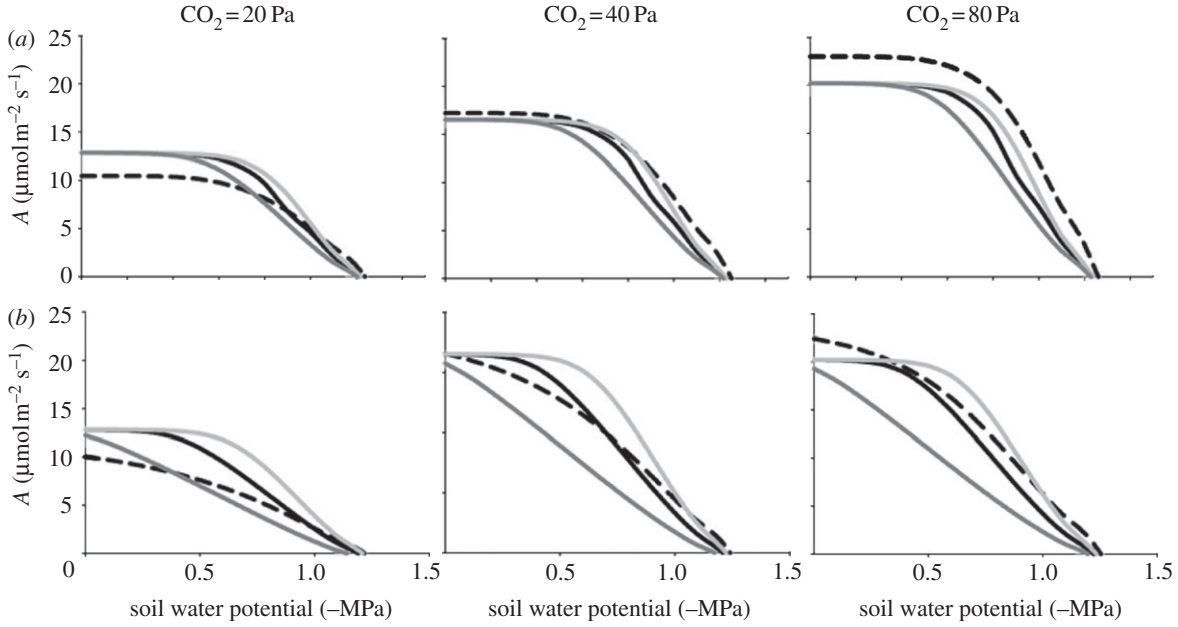

Figure 8. Simulated response of light-saturated photosynthetic rate to a drying soil at low (20 Pa), ambient (40 Pa) or high CO_2 (80 Pa) and VPD of (*a*) 1 kPa or (*b*) 3 kPa, for a C_3 species and C_4 grass species with identical plant hydraulic conductance (K_{plant}), and for a simulated C_4 species with double the K_{plant}, and a simulated C_4 species with half the K_{plant} (corresponding to its value of g_s being approximately half that of the C_3 species). (*a*,*b*) Dashed line, C_3; black solid line, C_4; light grey solid line, C_4, $2 \times K_{plant}$; dark grey solid line, C_4, $0.5 \times K_{plant}$.

species [91]. In contrast, when the C_4 species in our model simulations had reduced K_{plant}, this led to a much reduced value of A, and the C_3 species showed an advantage of A across all CO_2 levels as soil dried minimally (figure 8). These findings indicate that, theoretically, a reduced K_{plant} in C_4 species would annul any advantage of the C_4 pathway for photosynthesis under drought or low CO_2 in open environments. However, an equal or higher K_{plant} in these conditions would provide an advantage not only in maintaining open stomata, but also in maintaining a high A, providing a strong benefit to C_4 species.

What evidence is there that K_{plant} is high relative to g_s in C_4 compared with C_3 species? To-date, no studies have made the necessary direct experimental comparisons. Nonetheless, the two comparative studies of five C_3 and eight C_4 lineages of PACMAD grasses presented in figure 4*a* (a total of 40 different species) found that C_4 grasses generated a lower soil to leaf gradient in water potential ($\Delta\Psi$) during typical diurnal transpiration than closely related C_3 species [57,58]. Similar patterns have been observed for the C_3 and C_4 subspecies of *Alloteropsis semialata* in common garden plots at high irradiance and temperature [92]. This finding is consistent with the hypothesis of a higher ratio of hydraulic supply to demand, i.e. a greater K_{plant}/g_s in C_4 than C_3 grass species.

Notably, several studies of C_4 woody eudicots have suggested the opposite situation, measuring reduced stem hydraulic conductance per supplied leaf area (K_{stem}) relative to C_3 species [93–95]. This was hypothesized to evolve in the final stages of C_4 evolution after WUE has increased (table 1, phase 3). A reduced K_{stem} would not necessitate a reduction of g_s under well-watered conditions or mild drought. On the other hand, it would likely reduce xylem construction costs, and also possibly reduce the vulnerability to cavitation of stems, and thus their longevity [93–95]. Such adaptation would be especially important for the economics and protection of long-lived woody parts [93]. However, we note that a lower K_{stem} does not necessarily imply a lower K_{plant}; indeed, a higher leaf hydraulic conductance (K_{leaf}) can easily compensate. Recent work has shown the leaf is a critical bottleneck in the whole-plant hydraulic pathway, accounting for greater than 30 per cent of whole plant resistance, and that leaves have steeper hydraulic vulnerability curves than stem [96]. Consequently, K_{leaf} is a strong determinant of K_{plant}, especially when leaves begin to dehydrate during transpiration or incipient drought [97–101]. Such an importance of K_{leaf} in the whole plant pathway is thus consistent with a reduction of K_{stem} in woody dicot C_4 species. It is also consistent with the evolution of high vein density in C_3 species under drier climates (table 1, phase 1), which would serve to increase K_{leaf} and maintain or increase K_{plant}, while the evolution of higher water storage capacitance would buffer changes in leaf water potential during high VPD or drought [77,96,102,103]. These modifications would then be co-opted for further evolution of C_3–C_4 intermediates and C_4 species (table 1).

In §5, we argued that the low values of g_s in C_4 species save the hydraulic system from embolism, especially as leaves are heated in open environments, and as stomata are stimulated to open under low CO_2. Our model findings further show that the low values of g_s in C_4 species also reduce stomatal sensitivity to hydraulic feedbacks, allowing stomata to remain open during drought, and photosynthesis to continue, but only if C_4 species have similar or higher K_{plant} than C_3 species, and thus a high hydraulic supply relative to demand. A lower K_{plant} would serve to make C_4 species more sensitive to soil drought, especially under high VPD and low CO_2. The circumstantial evidence we have presented for grass species is consistent with our hypothesis for a high hydraulic supply relative to demand in C_4 species. However, to our knowledge, there are no published data comparing K_{leaf} for C_3 and C_4 plants in general, or for grasses specifically. Such data are essential to test our hypothesis.

7. METABOLIC LIMITATION OF PHOTOSYNTHESIS DURING SEVERE DROUGHT

We hypothesized that the evolution of the C_4 pathway provides significant physiological benefits for carbon-fixation and water conservation in well-watered soil, during the early stages of soil drought, or during transient drought events. However, there is no *a priori* reason to expect a greater tolerance of severe desiccation in C_4 than C_3 species [104]. In fact, recent comparative analyses of closely related C_3 and C_4 PACMAD grasses suggests the converse; that the C_4 photosynthetic system may be more prone to greater metabolic inhibition under chronic and severe drought events. Experimental evidence from controlled environment, common garden and field investigations all indicate that photosynthetic capacity declines to a greater extent with leaf water potential in C_4 than C_3 grass species after weeks of soil drying, or at very high VPD [57,92,105,106]. Chronic or severe drought may thus diminish, eliminate or even reverse the WUE advantage of C_4 over C_3 species. In the extreme case, photosynthetic capacity is significantly slower to recover after the end of the drought event [106]. Experimental evidence therefore suggests that metabolic limitation of photosynthesis will eventually offset hydraulic benefits of the C_4 syndrome during acute or prolonged drought events. For tolerance of severe drought, tight stomatal control and tissue water storage, as is strongly developed in CAM species, or desiccation-tolerant tissue, are far superior to C_4 metabolism. However, for tolerance of repeated transient droughts in the growing season, C_4 metabolism carries strong advantages, particularly under low CO_2.

8. CONCLUSIONS

We hypothesized that atmospheric CO_2 depletion coupled with high temperatures, open habitat and seasonally dry subtropical environments caused excessive demand for water transport, and selected for C_4 photosynthesis to enable lower stomatal conductance as a water-conserving mechanism. C_4 photosynthesis allowed high rates of carbon-fixation to be maintained

at low stomatal conductance, and reduced stomatal opening in response to low atmospheric CO_2. These mechanisms served to reduce strain on the hydraulic system. Maintaining a high hydraulic conductance enabled stomatal conductance and photosynthesis to be sustained for longer during drought events. The evolution of C_4 photosynthesis, therefore, rebalanced the fundamental trade-off between plant carbon and water relations, as atmospheric CO_2 declined in the geological past, and as ecological transitions drove increasing demand for water.

Our hypothesis adds the evolution of C_4 photosynthesis to the list of exceptional innovations based on the plant hydraulic system that arose during periods of low CO_2 that have impacted on plant life history, biogeography and the distribution of ecosystems in the deep past, present and future [107]. Previously hypothesized modifications of the water transport system and associated plant features driven by low CO_2 include the evolution of xylem vessels and stomata [108], and the planate leaf [109,110] with high vein density [78]. These innovations permitted more rapid growth and diversification, leading to the succession of dominance from pteridophytes to gymnosperms to angiosperms [78,80,111,112]. The evolution of C_4 photosynthesis, for improved performance in exposed, seasonally dry habitats in low CO_2, thus joins a long line of hydraulic innovations driven by low CO_2 that changed plants and the world.

We thank Nate McDowell, Brad Ripley, Jessica Pasquet-Kok and Christine Scoffoni for stimulating discussions on the role of photosynthetic pathway in plant hydraulics, Sam Taylor, Hui Liu and Mark Rees for help with the data analysis and presentation, and Rowan Sage and an anonymous reviewer for their insights and critical reviews of this paper. This work was inspired by the International Scientific Seminar 'Atmospheric CO_2 as a driver of plant evolution' organized by David Beerling at the Kavli Royal Society International Centre in September 2010, and we thank The Royal Society for funding and the opportunity to attend this meeting (C.P.O.). We also gratefully acknowledge funding for this work from a Royal Society University Research Fellowship (C.P.O.), NERC standard grant number NE/DO13062/1 (C.P.O.), and National Science Foundation Grant no. 0546784 (L.S.).

APPENDIX A

(a) *Model of evaporation from a leaf in a forest understorey or in open pasture*

The net radiation balance at the leaf surface (Φ_n) is a function of shortwave (S) and longwave (L) radiation fluxes (both W m^{-2}):

$$\Phi_n = S + L_d - 2L_l + L_s, \quad (A\,1)$$

where $2L_l$ represents longwave radiation emitted upwards and downwards from the leaf, L_s the upwards emission from soil and L_d the downwards emission from the sky or forest canopy, depending on tree cover. Values of L were calculated according to Stefan's Law, tracking the temperatures of leaf, soil, tree canopy and sky, by assuming that the lowest layer of leaves in the forest canopy is approximately at air temperature, and the apparent temperature of the clear sky is 20 K lower than that of surface air [113,114]. Heat storage by the leaf was assumed to be negligible, such that Φ_n is dissipated entirely via latent and sensible heat fluxes (λE and H, respectively)

$$\Phi_n = \lambda E + H. \quad (A\,2)$$

Evaporation from the leaf surface (E, mol H_2O m^{-2} s^{-1}) was modelled using two variants of the Penman–Monteith equation [115,116]. For the simulations shown in figure 3, we were interested in the potential for evapotranspiration in the absence of any limitation imposed by stomata, and used the original form [115]

$$E = \frac{\{s\,\Phi_n + \rho_a c_p g_a \mathrm{VPD}\}}{\lambda[s+\gamma]}, \quad (A\,3a),$$

where Φ_n is net radiation at the leaf surface (W m^{-2}), VPD is the atmospheric VPD (Pa), g_a is the leaf boundary layer conductance (m s^{-1}) and the remaining parameters are physical properties of air and water: s, the rate of change of saturation vapour pressure with temperature (Pa K^{-1}), ρ_a, the density of dry air (kg m^{-3}), c_p, the specific heat capacity of water (J kg^{-1} K^{-1}), γ, the psychrometer constant (Pa K^{-1}) and λ, the latent heat of evaporation for water (J mol^{-1}). The values of s, γ, ρ_a and λ were corrected for temperature following Friend [117]. We made the simplifying assumption that the leaf boundary layer conductance is approximately equal for heat and water.

For the simulations shown in figure 6, we were interested in the regulation of E by stomata, and used the modification by Monteith [116]:

$$E = \frac{\{s\,\Phi_n + \rho_a c_p g_a \mathrm{VPD}\}}{\lambda[s + (\gamma g_a / g_W)]}, \quad (A\,3b)$$

where g_W is the total leaf conductance for water:

$$g_W^{-1} = g_a^{-1} + g_s^{-1} \quad (A\,4)$$

and g_a is a function of leaf width ($d = 0.01$ m), and wind speed (u, m s^{-1}):

$$g_a = 6.62(u/d)^{0.5}. \quad (A\,5)$$

Values of g_s were prescribed for these simulations as a function of atmospheric CO_2, using the equations derived for C_3 and C_4 leaves in figure 5.

The sensible heat flux is given by:

$$H = (T_l - T_a)\rho_a c_p g_a, \quad (A\,6)$$

where T_l is the leaf temperature and T_a the air temperature (both K). To solve the leaf energy balance, equation (A 2) must be rearranged to give H, and equation (A 6) to give T_l:

$$H = \Phi_n - \lambda E \quad (A\,7)$$

and

$$T_l = T_a + \frac{H}{\rho_a c_p g_a}. \quad (A\,8)$$

Equations (A 1), (A 3), (A 7) and (A 8) are then solved simultaneously using iteration in R (The R

foundation for Statistical Computing) to yield values for Φ_n, E, H and T_l.

APPENDIX B

(a) Modelling of hydraulic-stomatal limitation on photosynthesis in C_3 and C_4 species

A model based on a few simplifying assumptions was used to determine the response of operating g_s and leaf water potential (Ψ_{leaf}) to declining soil water potential (Ψ_{soil}) and increasing vapour pressure deficit (VPD). The g_s was then used to estimate photosynthesis from a diffusion-biochemistry model (see appendix B). The hydraulic-stomatal model determines Ψ_{leaf}, plant hydraulic conductance (K_{plant}) and g_s at a given Ψ_{soil} and VPD. First, Ψ_{leaf} is determined based on steady-state water transport according to the Ohm's Law analogy [118,119]:

$$\Psi_{leaf} = \Psi_{soil} - \frac{(g_s \mathrm{VPD})}{K_{plant}}. \quad \text{(B 1)}$$

Secondly, a hydraulic response function modelled the vulnerability of K_{plant} to declining Ψ_{leaf}. This used a linear function to approximate observations between full hydration and turgor loss, as reported for the leaves of grasses and several other taxa [69,120,121]:

$$K_{plant} = K_{max} + a \times \Psi_{leaf}, \quad \text{(B 2)}$$

where K_{max} and a are constants for given species. We assumed that K_{plant} showed a similar vulnerability response to leaves [69,99], calculating $K_{plant} = 80\% \times$ leaf hydraulic conductance, based on the range shown in previous work on grasses (65% to over 80% of plant resistance in the leaf [69,101,118]). Changing these assumptions would not affect the comparative findings of our simulations.

Thirdly, we simulated the decline in g_s with more negative Ψ_{leaf} as a sigmoidal function:

$$g_s = \frac{g*}{1 + e^{-(\Psi_{leaf} - b)/c}}, \quad \text{(B 3)}$$

where $g*$ is the maximum value of g_s at $\Psi_{leaf} = 0$, and b is the Ψ_{leaf} at 50 per cent stomatal closure. The constant c defines the shape of the sigmoidal curve.

For given Ψ_{soil} and VPD, equations (B 1–B 3) were solved simultaneously, minimizing the implicit forms by iteration [122] (Microsoft Visual Basic; Microsoft, Redmond, WA, USA). Using this model, we simulated the response of g_s to Ψ_{soil} for C_3 and C_4 species, from 0 to −2 MPa, and at VPD of 1 and 3 kPa, using parameters for equations (B 1–B 3) from the literature, as available (table 2). We also tested scenarios for C_4 species with double the K_{plant} and half the K_{plant} of the C_3 species.

Table 2. Parameters used for hydraulic-stomatal-photosynthesis modelling.

parameter	units	C_3, C_4 values	source
leaf K_{max}	mmol m^{-2} s^{-1} MPa^{-1}	15, 15	[69]
a	mmol m^{-2} s^{-1} MPa^{-2}	−7.5, −7.5	[69]
$g*$	mol m^{-2} s^{-1}	0.25, 0.10	[58]
b	MPa	−1.0, −1.0	[69]
c	MPa	0.1, 0.1	[69,123]
$V_{c,\,max}$	μmol m^{-2} s^{-1}	83, 39	[124]
$\Gamma*$	μmol mol^{-1}	46, 10	[124]
K_c	μmol mol^{-1}	302, 302	[124]
K_o	μmol mol^{-1}	256, 256	[124]
O	mol mol^{-1}	0.210, 0.210	[124]
J_{max}	μmol m^{-2} s^{-1}	132, 180	[124]
R_d	μmol m^{-2} s^{-1}	1.66, 0.78	[124]
$V_{p,max}$	μmol m^{-2} s^{-1}	n.a., 120	[124]
K_p	μmol mol^{-1}	n.a., 80	[124]
V_{pr}	μmol m^{-2} s^{-1}	n.a., 80	[124]

(b) Modelling of photosynthetic rate from diffusion-biochemical limitations for C_3 and C_4 species during drought under varying vapour pressure deficit and atmospheric CO_2

We simulated photosynthetic rate (A) and its response to CO_2, by first modelling a direct response of g_s to CO_2, and then inputting the adjusted g_s values into equations for C_3 and C_4 photosynthesis.

First, for low and high CO_2 we multiplied the g_s values by a factor corresponding to 20 or 80 Pa (1.72 and 0.58, respectively) based on the data and fitted equations of figure 5. This multiplicative adjustment of g_s for CO_2 level was applied independently of the g_s response to water status (from which g_s was determined from equations (B 1–B 3) above). Thus, the model considers a simplified scenario in which the response of stomata to VPD and soil drought on one hand, and to CO_2 on the other, is independent and multiplicative, with no hydraulic or hormonal feedback on g_s. The assumption is consistent with previous work measuring the effects of CO_2 and VPD on g_s in C_3 and C_4 species [68]. This independence of the responses would put plants in low CO_2 at risk of severe leaf dehydration if stomata open strongly when VPD is low, and, indeed, such dehydration has been observed [125]. However, there is evidence that declining soil water availability can interact with the CO_2 response, resulting in greater sensitivity of stomata to CO_2, to a varying degree across different C_3 and C_4 species, in part modulated by abscisic acid responsiveness [126,127]. More work is needed to resolve and to explicitly model the potential interactions of stomatal responses to different factors in C_3 and C_4 species. For example, the interaction with falling soil water potential during drought would be expected to produce a stronger decline of g_s and of A.

In our model, the g_s, now adjusted for CO_2, was used to predict A based on the equations for C_3 and C_4 photosynthesis provided by von Caemmerer [29], using parameters from Vico & Porporato [124] (table 2). We assumed that the impact of Ψ_{leaf} on A was mediated by g_s without any separate, direct impacts on mesophyll conductance or on metabolism itself; these impacts could be added but, without detailed information of differential impacts on C_3 and C_4 species, would not change the outcome of our scenarios [124].

Thus, for C_3 species, A was determined as

$$A = \min(A_c, A_j) - R_d, \quad \text{(B 4)}$$

where A_c is the Rubisco-limited rate of photosynthesis, A_j is the rate of RuBP-limited CO_2 assimilation and R_d

is the total mitochondrial rate of respiration. In turn,

$$A_c = V_{c,max}\frac{C_m - \Gamma^*}{C_m + K_c(1 + (O/K_o))}, \quad \text{(B 5)}$$

where $V_{c,max}$ is the maximum catalytic activity of Rubisco at current leaf temperature (here considered as optimal); C_m is the CO_2 concentration at the site of photosynthesis in the mesophyll cell (MC); Γ^* is the equilibrium CO_2 compensation point for gross photosynthesis; K_c and K_o are the coefficients for CO_2 and O_2 of the Michaelis–Menten kinetics, accounting for competitive inhibition by O_2; and O is the O_2 concentration at the site of photosynthesis.

$$A_J = J_{max}\frac{C_m - \Gamma^*}{4(C_m + 2\Gamma^*)}, \quad \text{(B 6)}$$

where J_{max} is the maximum potential rate of electron transport. To determine A, the equations (B 5) and (B 6) were each equated separately with the diffusion equation:

$$A = (C_a - C_m) \times g_t, \quad \text{(B 7)}$$

where C_a is the atmospheric CO_2 concentration. The value of g_t was determined as the conductance to CO_2 from the atmosphere to the intercellular space (stomatal conductance to CO_2, g_{s,CO_2}) and from the intercellular space to the chloroplast (mesophyll conductance, g_m) in series:

$$\frac{1}{g_t} = \frac{1}{g_{s,CO_2}} + \frac{1}{g_m}, \quad \text{(B 8)}$$

where g_{s,CO_2} was determined as $g_s/1.6$ and g_m as $g_s \times 1.65$ [124]. In each case (equations B 6 = B 8, and equations B 7 = B 8), the equations were solved for a given g_s and C_a, to determine C_m using the quadratic equation. The values of C_m were inserted into equations (B 5) and (B 6), respectively, to determine A_c and A_j, before applying equation (B 4) to determine A.

For the C_4 species, a similar approach was used, but the first step involved determining the PEP carboxylation rate (V_p):

$$V_p = \min\left(\frac{C_m V_{p,max}}{C_m + K_p}, V_{pr}\right), \quad \text{(B 9)}$$

where $V_{p,max}$ is the maximum rate of PEP carboxylation, V_{pr} is an upper bound set by PEP regeneration rate and K_p is the Michaelis–Menten coefficient of PEPC. The C_m was determined by equating equation (B 9) with equation (B 7) for a given C_a and g_s. We then used the C_m and V_p to determine the A, by combining two equations:

$$A = V_p - L_{bs} - R_d, \quad \text{(B 10)}$$

where L_{bs} is bundle sheath leakage, given by:

$$L_{bs} = g_{bs}(C_{bs} - C_m), \quad \text{(B 11)}$$

and C_{bs} is the CO_2 concentration in the bundle sheath. Substituting equation (B 11) into equation (B 10), and making this equation equal to each of equations (B 5) and (B 6) separately (substituting C_{bs} for C_m in those equations), allowed them to be solved for C_{bs}. Equations (B 5) and (B 6) were then used to determine A_c and A_j, and equation (B 4) to determine A.

REFERENCES

1 Hohmann-Marriott, M. F. & Blankenship, R. E. 2011 Evolution of photosynthesis. *Annu. Rev. Plant Biol.* **441**, 940–941. (doi:10.1146/annurev-arplant-042110-103811)

2 Crayn, D. M., Winter, K. & Smith, J. A. C. 2004 Multiple origins of crassulacean acid metabolism and the epiphytic habit in the Neotropical family Bromeliaceae. *Proc. Natl Acad. Sci. USA* **101**, 3703–3708. (doi:10.1073/pnas.0400366101)

3 Edwards, E. J., Osborne, C. P., Strömberg, C. A. E., Smith, S. A. & C_4 Grasses Consortium. 2010 The origins of C_4 grasslands: integrating evolutionary and ecosystem science. *Science* **328**, 587–591. (doi:10.1126/science.1177216)

4 Beerling, D. J. & Royer, D. L. 2011 Convergent cenozoic CO_2 history. *Nat. Geosci.* **4**, 418–420. (doi:10.1038/ngeo1186)

5 Young, J. N., Rickaby, R. E. M., Kapralov, M. V. & Filatov, D. A. 2012 Adaptive signals in algal Rubisco reveal a history of ancient atmospheric carbon dioxide. *Phil Trans. R. Soc. B* **367**, 483–492. (doi:10.1098/rstb.2011.0145)

6 Osmond, C. B., Troughton, J. H. & Goodchild, D. J. 1969 Physiological, biochemical and structural studies of photosynthesis and photorespiration in two species of *Atriplex*. *Zeit. Pflanzenphysiol.* **61**, 218–237.

7 Berry, J. A., Downton, W. J. S. & Tregunna, E. B. 1970 The photosynthetic carbon metabolism of *Zea mays* and *Gomphrena globosa:* the location of the CO_2 fixation and carboxyl transfer reactions. *Can. J. Bot.* **48**, 777–786. (doi:10.1139/b70-106)

8 Voznesenskaya, E. V., Franceschi, V. R., Kiirats, O., Freitag, H. & Edwards, G. E. 2001 Kranz anatomy is not essential for terrestrial C_4 plant photosynthesis. *Nature* **414**, 543–546. (doi:10.1038/35107073)

9 Watson, L. & Dallwitz, M. J. 1992 The grass genera of the world: descriptions, illustrations, identification, and information retrieval; including synonyms, morphology, anatomy, physiology, phytochemistry, cytology, classification, pathogens, world and local distribution, and references. Version: 25th November 2008. See http://delta-intkey.com.

10 Cerling, T. E., Harris, J. M., MacFadden, B. J., Leakey, M. G., Quade, J., Eisenmann, V. & Ehleringer, J. R. 1997 Global vegetation change through the Miocene/Pliocene boundary. *Nature* **389**, 153–158. (doi:10.1038/38229)

11 Ehleringer, J. R., Cerling, T. E. & Helliker, B. R. 1997 C_4 photosynthesis, atmospheric CO_2, and climate. *Oecologia* **112**, 285–299. (doi:10.1007/s004420050311)

12 Hatch, M. D., Osmond, C. B. & Slatyer, R. O. (eds) 1971 *Photosynthesis and photorespiration.* New York, NY: Wiley-Interscience.

13 Bräutigam, A. *et al.* 2011 An mRNA blueprint for C_4 photosynthesis derived from comparative transcriptomics of closely related C_3 and C_4 species. *Plant Physiol.* **155**, 142–156. (doi:10.1104/pp.110.159442)

14 Brown, N. J., Newell, C. A., Stanley, S., Chen, J. E., Perrin, A. J., Kajala, K. & Hibberd, J. M. 2011 Independent and parallel recruitment of preexisting mechanisms underlying C_4 photosynthesis. *Science* **331**, 1436–1439. (doi:10.1126/science.1201248)

15 Christin, P. A., Salamin, N., Savolainen, V., Duvall, M. R. & Besnard, G. 2007 C_4 photosynthesis evolved

in grasses via parallel adaptive genetic changes. *Curr. Biol.* **17**, 1241–1247. (doi:10.1016/j.cub.2007.06.036)
16 Sage, R. F., Christin, P. A. & Edwards, E. J. 2011 The C_4 lineages of planet Earth. *J. Exp. Bot.* **62**, 3155–3169. (doi:10.1093/jxb/err048)
17 Westhoff, P. & Govik, U. 2010 Evolution of C_4 photosynthesis—looking for the master switch. *Plant Physiol.* **154**, 598–601. (doi:10.1104/pp.110.161729)
18 Hibberd, J. M. & Quick, W. P. 2002 Characteristics of C_4 photosynthesis in stems and petioles of C_3 flowering plants. *Nature* **415**, 451–454. (doi:10.1038/415451a)
19 Sage, R. F. 2004 The evolution of C_4 photosynthesis. *New Phytol.* **161**, 341–370. (doi:10.1111/j.1469-8137.2004.00974.x)
20 Hibberd, J. M. & Covshoff, S. 2010 The regulation of gene expression required for C_4 photosynthesis. *Annu. Rev. Plant Biol.* **61**, 181–207. (doi:10.1146/annurev-arplant-042809-112238)
21 Christin, P. A., Freckleton, R. P. & Osborne, C. P. 2010 Can phylogenetics identify C_4 origins and reversals? *Trends Ecol. Evol.* **25**, 403–409. (doi:10.1016/j.tree.2010.04.007)
22 Ehleringer, J. R., Sage, R. F., Flanagan, L. B. & Pearcy, R. W. 1991 Climate change and the evolution of C_4 photosynthesis. *Trends Ecol. Evol.* **6**, 95–99. (doi:10.1016/0169-5347(91)90183-X)
23 Griffiths, H. 2006 Plant biology: designs on Rubisco. *Nature* **441**, 940–941. (doi:10.1038/441940a)
24 Tcherkez, G. G. B., Farquhar, G. D. & Andrews, T. J. 2006 Despite slow catalysis and confused substrate specificity, all ribulose bisphosphate carboxylases may be nearly perfectly optimized. *Proc. Natl Acad. Sci. USA* **103**, 7246–7251. (doi:10.1073/pnas.0600605103)
25 Long, S. P. 1991 Modification of the response of photosynthetic productivity to rising temperature by atmospheric CO_2 concentrations: has its importance been underestimated? *Plant Cell Environ.* **14**, 729–739. (doi:10.1111/j.1365-3040.1991.tb01439.x)
26 Furbank, R. T. & Hatch, M. D. 1987 Mechanism of C_4 photosynthesis. The size and composition of the inorganic carbon pool in bundle sheath cells. *Plant Physiol.* **85**, 958–964. (doi:10.1104/pp.85.4.958)
27 Ehleringer, J. & Björkman, O. 1977 Quantum yields for CO_2 uptake in C_3 and C_4 plants. Dependence on temperature, CO_2, and O_2 concentration. *Plant Physiol.* **59**, 86–90. (doi:10.1104/pp.59.1.86)
28 Ehleringer, J. & Pearcy, R. W. 1983 Variation in quantum yield for CO_2 uptake among C_3 and C_4 plants. *Plant Physiol.* **73**, 555–559. (doi:10.1104/pp.73.3.555)
29 von Caemmerer, S. 2000 *Biochemical models of leaf photosynthesis*. Victoria, Australia: CSIRO Publishing.
30 Cunniff, J., Osborne, C. P., Ripley, B. S., Charles, M. & Jones, G. 2008 Response of wild C_4 crop progenitors to sub-ambient CO_2 highlights a possible role in the origin of agriculture. *Glob. Change Biol.* **14**, 576–587. (doi:10.1111/j.1365-2486.2007.01515.x)
31 Long, S. P. 1999 Environmental responses. In *C_4 plant biology* (eds R. F. Sage & R. K. Monson), pp. 215–249. San Diego, CA: Academic Press.
32 Ehleringer, J. 1978 Implications of quantum yield differences to the distributions of C_3 and C_4 plants. *Oecologia* **31**, 255–267. (doi:10.1007/BF00346246)
33 Robichaux, R. H. & Pearcy, R. W. 1984 Evolution of C_3 and C_4 plants along an environmental moisture gradient: patterns of photosynthetic differentiation in Hawaiian *Scaevola* and *Euphorbia* species. *Am. J. Bot.* **71**, 121–129. (doi:10.2307/2443631)
34 Ehleringer, J. R. & Monson, R. K. 1993 Evolutionary and ecological aspects of photosynthetic pathway variation. *Annu. Rev. Ecol. Syst.* **24**, 411–439. (doi:10.1146/annurev.es.24.110193.002211)
35 Christin, P. A., Osborne, C. P., Sage, R. F., Arakaki, M. & Edwards, E. J. 2011 C_4 eudicots are not younger than C_4 monocots. *J. Exp. Bot.* **62**, 3171–3181. (doi:10.1093/jxb/err041)
36 Christin, P. A., Besnard, G., Samaritani, E., Duvall, M. R., Hodkinson, T. R., Savolainen, V. & Salamin, N. 2008 Oligocene CO_2 decline promoted C_4 photosynthesis in grasses. *Curr. Biol.* **18**, 37–43. (doi:10.1016/j.cub.2007.11.058)
37 Vicentini, A., Barber, J. C., Aliscioni, A. S., Giussani, A. M. & Kellogg, E. A. 2008 The age of the grasses and clusters of origins of C_4 photosynthesis. *Glob. Change Biol.* **14**, 2963–2977. (doi:10.1111/j.1365-2486.2008.01688.x)
38 Teeri, J. A. & Stowe, L. G. 1976 Climatic patterns and the distribution of C_4 grasses in North America. *Oecologia* **23**, 1–12. (doi:10.1007/BF00351210)
39 Rundel, P. W. 1980 The ecological distribution of C_4 and C_3 grasses in the Hawaiian Islands. *Oecologia* **45**, 354–359. (doi:10.1007/BF00540205)
40 Edwards, E. J. & Still, C. J. 2008 Climate, phylogeny and the ecological distribution of C_4 grasses. *Ecol. Lett.* **11**, 266–276. (doi:10.1111/j.1461-0248.2007.01144.x)
41 Edwards, E. J. & Smith, S. A. 2010 Phylogenetic analyses reveal the shady history of C_4 grasses. *Proc. Natl Acad. Sci. USA* **107**, 2532–2537. (doi:10.1073/pnas.0909672107)
42 Osborne, C. P. & Freckleton, R. P. 2009 Ecological selection pressures for C_4 photosynthesis in the grasses. *Proc. R. Soc. B* **276**, 1753–1760. (doi:10.1098/rspb.2008.1762)
43 Kellogg, E. A. 2001 Evolutionary history of the grasses. *Plant Physiol.* **125**, 1198–1205. (doi:10.1104/pp.125.3.1198)
44 Schulze, E.-D., Ellis, R., Schulze, W., Trimborn, P. & Ziegler, H. 1996 Diversity, metabolic types and ^{13}C carbon isotope ratios in the grass flora of Namibia in relation to growth form, precipitation and habitat conditions. *Oecologia* **106**, 352–369. (doi:10.1007/BF00334563)
45 Ruddiman, W. J. 2007 *Earth's Climate: past and future*, 2nd edn. New York, NY: W. H. Freeman.
46 Pound, M. J., Haywood, A. M., Salzmann, U., Riding, J. B., Lunt, D. J. & Hunter, S. J. 2011 A Tortonian (Late Miocene, 11.61–7.25 Ma) global vegetation reconstruction. *Palaeogeogr. Palaeoclimatol. Palaeoecol.* **300**, 29–45. (doi:10.1016/j.palaeo.2010.11.029)
47 Sankaran, M. *et al.* 2005 Determinants of woody cover in African savannas. *Nature* **438**, 846–849. (doi:10.1038/nature04070)
48 Tipple, B. J. & Pagani, M. 2007 The early origins of terrestrial C_4 photosynthesis. *Annu. Rev. Earth Planet Sci.* **35**, 435–461. (doi:10.1146/annurev.earth.35.031306.140150)
49 Lehmann, C. E. R., Archibald, S. A., Hoffmann, W. A. & Bond, W. J. 2011 Deciphering the distribution of the savanna biome. *New Phytol.* **191**, 197–209. (doi:10.1111/j.1469-8137.2011.03689.x)
50 Beerling, D. J. 1999 New estimates of carbon transfer to terrestrial ecosystems between the last glacial maximum and the Holocene. *Terra Nova* **11**, 162–167. (doi:10.1046/j.1365-3121.1999.00240.x)
51 Bond, W. J. & Midgley, G. F. 2000 A proposed CO_2-controlled mechanism of woody plant invasion in grasslands and savannas. *Glob. Change Biol.* **6**, 865–869. (doi:10.1046/j.1365-2486.2000.00365.x)
52 Beerling, D. J. & Osborne, C. P. 2006 The origin of the savannah biome. *Glob. Change Biol.* **12**, 2023–2031. (doi:10.1111/j.1365-2486.2006.01239.x)
53 Bond, W. J. & Midgley, G. F. 2012 Carbon dioxide and the uneasy interactions of trees and savannah grasses.

Phil Trans. R. Soc. B **367**, 601–612. (doi:10.1098/rstb.2011.0182)
54 Williams-Linera, G., Domínguez-Gastelú, V. & García-Zurita, M. E. 1998 Microenvironment and floristics of different edges in a fragmented tropical rainforest. *Conserv. Biol.* **12**, 1091–1102. (doi:10.1046/j.1523-1739.1998.97262.x)
55 Davies-Colley, R. J., Payne, G. W. & van Elswijk, M. 2000 Microclimate gradients across a forest edge. *New Zeal. J. Ecol.* **24**, 111–121.
56 Buckley, T. N. 2005 The control of stomata by water balance. *New Phytol.* **168**, 275–292. (doi:10.1111/j.1469-8137.2005.01543.x)
57 Taylor, S. H., Ripley, B. S., Woodward, F. I. & Osborne, C. P. 2011 Drought limitation of photosynthesis differs between C_3 and C_4 grass species in a comparative experiment. *Plant Cell Environ.* **34**, 65–75. (doi:10.1111/j.1365-3040.2010.02226.x)
58 Taylor, S. H., Hulme, S. P., Rees, M., Ripley, B. S., Woodward, F. I. & Osborne, C. P. 2010 Ecophysiological traits in C_3 and C_4 grasses: a phylogenetically controlled screening experiment. *New Phytol.* **185**, 780–791. (doi:10.1111/j.1469-8137.2009.03102.x)
59 Farquhar, G. D., von Caemmerer, S. & Berry, J. A. 1980 A biochemical model of photosynthetic CO_2 assimilation in leaves of C_3 species. *Planta* **149**, 78–90. (doi:10.1007/BF00386231)
60 Downes, R. W. 1969 Differences in transpiration rates between tropical and temperate grasses under controlled conditions. *Planta* **88**, 261–273. (doi:10.1007/BF00385069)
61 Pearcy, R. W. & Ehleringer, J. 1983 Comparative ecophysiology of C_3 and C_4 plants. *Plant Cell Environ.* **7**, 1–13. (doi:10.1111/j.1365-3040.1984.tb01194.x)
62 Ward, J. K., Tissue, D. T., Thomas, R. B. & Strain, B. R. 1999 Comparative responses of model C_3 and C_4 plants to drought in low and elevated CO_2. *Glob. Change Biol.* **5**, 857–867. (doi:10.1046/j.1365-2486.1999.00270.x)
63 Cowling, S. A. & Sage, R. F. 1998 Interactive effects of low atmospheric CO_2 and elevated temperature on growth, photosynthesis and respiration in *Phasaeolus vulgaris*. *Plant Cell Environ.* **21**, 427–435. (doi:10.1046/j.1365-3040.1998.00290.x)
64 Anderson, L. J., Maherali, H., Johnson, H. B., Polley, H. W. & Jackson, R. B. 2001 Gas exchange and photosynthetic acclimation over subambient to elevated CO_2 in a C_3–C_4 grassland. *Glob. Change Biol.* **7**, 693–707. (doi:10.1046/j.1354-1013.2001.00438.x)
65 Pinto, H., Tissue, D. T. & Ghannoum, O. 2011 *Panicum milioides* (C_3–C_4) does not have improved water or nitrogen economies relative to C_3 and C_4 congeners exposed to industrial-age climate change. *J. Exp. Bot.* **62**, 3223–3234 (doi:10.1093/jxb/err005)
66 Wand, S. J. E., Midgley, G. F., Jones, M. H. & Curtis, P. S. 1999 Responses of wild C_4 and C_3 grass (Poaceae) species to elevated atmospheric CO_2 concentration: a meta-analytic test of current theories and perceptions. *Glob. Change Biol.* **5**, 723–741. (doi:10.1046/j.1365-2486.1999.00265.x)
67 Ainsworth, E. A. & Rogers, A. 2007 The response of photosynthesis and stomatal conductance to rising [CO_2]: mechanisms and environmental interactions. *Plant Cell Environ.* **30**, 258–270. (doi:10.1111/j.1365-3040.2007.01641.x)
68 Morison, J. I. L. & Gifford, R. M. 1983 Stomatal sensitivity to carbon dioxide and humidity: a comparison of two C_3 and two C_4 grass species. *Plant Physiol.* **71**, 789–796. (doi:10.1104/pp.71.4.789)
69 Holloway-Phillips, M.-M. & Brodribb, T. J. 2011 Minimum hydraulic safety leads to maximum water-use efficiency in a forage grass. *Plant Cell Environ.* **34**, 302–313. (doi:10.1111/j.1365-3040.2010.02244.x)
70 Muhaidat, R., Sage, T. L., Frohlich, M. W., Dengler, N. G. & Sage, R. F. 2011 Characterization of C_3-C_4 intermediate species in the genus *Heliotropium* L. (Boraginaceae): anatomy, ultrastructure and enzyme activity. *Plant Cell Environ.* **34**, 1723–1736. (doi:10.1111/j.1365-3040.2011.02367.x)
71 Sage, R. F. 2001 Environmental and evolutionary preconditions for the origin and diversification of the C_4 photosynthetic syndrome. *Plant Ecol.* **3**, 202–213. (doi:10.1055/s-2001-15206)
72 McKown, A. D. & Dengler, N. G. 2007 Key innovations in the evolution of Kranz anatomy and C_4 vein pattern in *Flaveria* (Asteraceae). *Am. J. Bot.* **94**, 382–399. (doi:10.3732/ajb.94.3.382)
73 McDowell, N. G. *et al.* 2008 Mechanisms of plant survival and mortality during drought: why do some plants survive whilst others succumb to drought? *New Phytol.* **178**, 719–739. (doi:10.1111/j.1469-8137.2008.02436.x)
74 McDowell, N. G. 2011 Mechanisms linking drought, hydraulics, carbon metabolism, and vegetation mortality. *Plant Physiol.* **155**, 1051–1059. (doi:10.1104/pp.110.170704)
75 Campbell, C. D., Sage, R. F., Kocacinar, F. & Way, D. A. 2005 Estimation of the whole-plant CO_2 compensation point of tobacco (*Nicotiana tabacum* L.). *Glob. Change Biol.* **11**, 1956–1967. (doi:10.1111/j.1365-2486.2005.01045.x)
76 Uhl, D. & Mosbrugger, V. 1999 Leaf venation density as a climate and environmental proxy: a critical review and new data. *Paleogeogr. Paleoclimatol. Paleoecol.* **149**, 15–26. (doi:10.1016/S0031-0182(98)00189-8)
77 Sack, L. & Frole, K. 2006 Leaf structural diversity is related to hydraulic capacity in tropical rain forest trees. *Ecology* **87**, 483–491. (doi:10.1890/05-0710)
78 Brodribb, T. J. & Feild, T. S. 2010 Leaf hydraulic evolution led a surge in leaf photosynthetic capacity during early angiosperm diversification. *Ecol. Lett.* **13**, 175–183. (doi:10.1111/j.1461-0248.2009.01410.x)
79 Dunbar-Co, S., Sporck, M. J. & Sack, L. 2009 Leaf trait diversification and design in seven rare taxa of the Hawaiian *Plantago* radiation. *Int. J. Plant Sci.* **170**, 61–75. (doi:10.1086/593111)
80 Feild, T. S. *et al.* 2011 Fossil evidence for Cretaceous escalation in angiosperm leaf vein evolution. *Proc. Natl Acad. Sci. USA* **108**, 8363–8366. (doi:10.1073/pnas.1014456108)
81 Ogle, K. 2003 Implications of interveinal distance for quantum yield in C_4 grasses: a modeling and meta-analysis. *Oecologia* **136**, 532–542. (doi:10.1007/s00442-003-1308-2)
82 McKown, A. D. & Dengler, N. G. 2010 Vein patterning and evolution in C_4 plants. *Botany-Botanique* **88**, 775–786. (doi:10.1139/B10-055)
83 Philpott, J. 1953 A blade tissue study of leaves of 47 species of *Ficus*. *Bot. Gaz.* **115**, 15–35. (doi:10.1086/335794)
84 Fisher, D. D., Schenk, H. J., Thorsch, J. A. & Ferren, W. R. 1997 Leaf anatomy and subgeneric affiliations of C_3 and C_4 species of *Suaeda* (Chenopodiaceae) in North America. *Am. J. Bot.* **84**, 1198–1210. (doi:10.2307/2446043)
85 Boughton, V. H. 1986 Phyllode structure, taxonomy and distribution in some Australian Acacias. *Aust. J. Bot.* **34**, 663–674. (doi:10.1071/BT9860663)
86 Voznesenskaya, E. V., Koteyeva, N. K., Edwards, G. E. & Ocampo, G. 2010 Revealing diversity in structural and biochemical forms of C_4 photosynthesis and a C_3-C_4

intermediate in genus *Portulaca* L. (Portulacaceae). *J. Exp. Bot.* **61**, 3647–3662. (doi:10.1093/jxb/erq178)
87 Arakaki, M., Christin, P.-A., Nyffeler, R., Lendel, A., Eggli, U., Ogburn, R. M., Spriggs, E., Moore, M. J. & Edwards, E. J. 2011 Contemporaneous and recent radiations of the world's major succulent plant lineages. *Proc. Natl Acad. Sci. USA* **108**, 8379–8384. (doi:10.1073/pnas.1100628108)
88 Vogan, P. J., Frohlich, M. W. & Sage, R. F. 2007 The functional significance of C3-C4 intermediate traits in *Heliotropium* L. (Boraginaeae): gas exchange perspectives. *Plant Cell Environ.* **10**, 1337–1345. (doi:10.1111/j.1365-3040.2007.01706.x)
89 Monson, R. K., Schuster, W. S. & Ku, M. S. B. 1987 Photosynthesis in *Flaveria brownii* A.M. Powell. A C_4-like C_3-C_4 intermediate. *Plant Physiol.* **85**, 1063–1067. (doi:10.1104/pp.85.4.1063)
90 Gong, C. M., Bai, J., Deng, J. M., Wang, G. X. & Liu, X. P. 2011 Leaf anatomy and photosynthetic carbon metabolic characteristics in *Phragmites communis* in different soil water availability. *Plant Ecol.* **212**, 675–687. (doi:10.1007/s11258-010-9854-2)
91 Schulze, E.-D. & Hall, A. E. 1982 Stomatal responses, water loss and CO_2 assimilation rates of plants in contrasting environments. In *Encyclopedia of plant physiology, vol. 12B: physiological plant ecology II: Water relations and carbon asssimilation* (eds O. L. Lange, P. S. Nobel, C. B. Osmond & H. Ziegler), Berlin, Germany: Springer.
92 Ibrahim, D. G., Gilbert, M. E., Ripley, B. S. & Osborne, C. P. 2008 Seasonal differences in photosynthesis between the C_3 and C_4 subspecies of *Alloteropsis semialata* are offset by frost and drought. *Plant Cell Environ.* **31**, 1038–1050. (doi:10.1111/j.1365-3040.2008.01815.x)
93 Kocacinar, F. & Sage, R. F. 2003 Photosynthetic pathway alters xylem structure and hydraulic function in herbaceous plants. *Plant Cell Environ.* **26**, 2015–2026. (doi:10.1111/j.1365-2478.2003.01119.x)
94 Kocacinar, F. & Sage, R. F. 2004 Photosynthetic pathway alters hydraulic structure and function in woody plants. *Oecologia* **139**, 214–223. (doi:10.1007/s00442-004-1517-3)
95 Kocacinar, F., McKown, A. D., Sage, T. L. & Sage, R. F. 2008 Photosynthetic pathway influences xylem structure and function in *Flaveria* (Asteraceae). *Plant Cell Environ.* **31**, 1363–1376. (doi:10.1111/j.1365-3040.2008.01847.x)
96 Sack, L., Cowan, P. D., Jaikumar, N. & Holbrook, N. M. 2003 The 'hydrology' of leaves: co-ordination of structure and function in temperate woody species. *Plant Cell Environ.* **26**, 1343–1356. (doi:10.1046/j.0016-8025.2003.01058.x)
97 Sack, L. & Holbrook, N. M. 2006 Leaf hydraulics. *Annu. Rev. Plant Biol.* **57**, 361–381. (doi:10.1146/annurev.arplant.56.032604.144141)
98 Brodribb, T. J. 2009 Xylem hydraulic physiology: the functional backbone of terrestrial plant productivity. *Plant Sci.* **177**, 245–251. (doi:10.1016/j.plantsci.2009.06.001)
99 Brodribb, T. J. & Cochard, H. 2009 Hydraulic failure defines the recovery and point of death in water stressed conifers. *Plant Physiol.* **149**, 575–584. (doi:10.1104/pp.108.129783)
100 Johnson, D. M., McCulloh, K. A., Meinzer, F. C., Woodruff, D. R. & Eissenstat, D. M. 2011 Hydraulic patterns and safety margins, from stem to stomata, in three eastern US tree species. *Tree Physiol.* **31**, 659–668. (doi:10.1093/treephys/tpr050)
101 Martre, P., Cochard, H. & Durand, J. L. 2001 Hydraulic architecture and water flow in growing grass tillers (*Festuca arundinacea* Schreb.). *Plant Cell Environ.* **24**, 65–76. (doi:10.1046/j.1365-3040.2001.00657.x)
102 Brodribb, T. J., Feild, T. S. & Jordan, G. J. 2007 Leaf maximum photosynthetic rate and venation are linked by hydraulics. *Plant Physiol.* **144**, 1890–1898. (doi:10.1104/pp.107.101352)
103 McKown, A. D., Cochard, H. & Sack, L. 2010 Decoding leaf hydraulics with a spatially explicit model: principles of venation architecture and implications for its evolution. *Am. Nat.* **175**, 447–460. (doi:10.1086/650721)
104 Osmond, C. B., Winter, K. & Ziegler, H. 1982 Functional significance of different pathways of CO_2 fixation in photosynthesis. In *Encyclopedia of plant physiology: new series* (eds O. L. Lange, P. S. Nobel, C. B. Osmond & H. Ziegler), pp. 479–547. Berlin, Germany: Springer.
105 Ripley, B. S., Gilbert, M. E., Ibrahim, D. G. & Osborne, C. P. 2007 Drought constraints on C_4 photosynthesis: stomatal and metabolic limitations in C_3 and C_4 subspecies of *Alloteropsis semialata*. *J. Exp. Bot.* **58**, 1351–1363. (doi:10.1093/jxb/erl302)
106 Ripley, B., Frole, K. & Gilbert, M. E. 2010 Differences in drought sensitivities and photosynthetic limitations between co-occurring C_3 and C_4 (NADP-ME) Panicoid grasses. *Ann. Bot.* **105**, 493–503. (doi:10.1093/aob/mcp307)
107 Leakey, A. D. B. & Lau, J. A. 2012 Evolutionary context for understanding and manipulating plant responses to past, present and future atmospheric [CO_2]. *Phil Trans. R. Soc. B* **367**, 613–629. (doi:10.1098/rstb.2011.0248)
108 Sperry, J. S. 2003 Evolution of water transport and xylem structure. *Int. J. Plant Sci.* **164**, S115–S127. (doi:10.1086/368398)
109 Beerling, D. J., Osborne, C. P. & Chaloner, W. G. 2001 Evolution of leaves in land plants linked to atmospheric CO_2 decline in the Late Palaeozoic era. *Nature* **410**, 352–354. (doi:10.1038/35066546)
110 Osborne, C. P., Beerling, D. J., Lomax, B. H. & Chaloner, W. G. 2004 Biophysical constraints on the origin of leaves inferred from the fossil record. *Proc. Natl Acad. Sci. USA* **101**, 10 360–10 362. (doi:10.1073/pnas.0402787101)
111 Bond, W. J. 1989 The tortoise and the hare: ecology of angiosperm dominance and gymnosperm persistence. *Biol. J. Linn. Soc.* **36**, 227–249. (doi:10.1111/j.1095-8312.1989.tb00492.x)
112 Haworth, M., Elliott-Kingston, C. & McElwain, J. C. 2011 Stomatal control as a driver of plant evolution. *J. Exp. Bot.* **62**, 2419–2423. (doi:10.1093/jxb/err086)
113 Monteith, J. L. & Unsworth, M. 1990 *Principles of environmental physics*, p. 291. London, UK: Edward Arnold.
114 Jones, H. G. 1992 *Plants and microclimate*, p. 428, 2nd edn. Cambridge, UK: Cambridge University Press.
115 Penman, H. L. 1948 Natural evaporation from open water, bare soil and grass. *Proc. R. Soc. Lond. A* **194**, 120–145. (doi:10.1098/rspa.1948.0037)
116 Monteith, J. L. 1965 Evaporation and environment. *Symp. Soc. Exp. Biol.* **19**, 205–234.
117 Friend, A. D. 1995 PGEN - an integrated model of leaf photosynthesis, transpiration, and conductance. *Ecol. Model.* **77**, 233–255. (doi:10.1016/0304-3800(93)E0082-E)
118 Wei, C. F., Tyree, M. T. & Steudle, E. 1999 Direct measurement of xylem pressure in leaves of intact maize plants. A test of the cohesion-tension theory

taking hydraulic architecture into consideration. *Plant Physiol.* **121**, 1191–1205. (doi:10.1104/pp.121.4.1191)
119 Tyree, M. T. & Zimmermann, M. H. 2002 *Xylem structure and the ascent of sap.* Berlin, Germany: Springer.
120 Brodribb, T. J. & McAdam, S. A. M. 2011 Passive origins of stomatal control in vascular plants. *Science* **331**, 582–585. (doi:10.1126/science.1197985)
121 Scoffoni, C., Rawls, M., McKown, A. D., Cochard, H. & Sack, L. 2011 Decline of leaf hydraulic conductance with dehydration: relationship to leaf size and venation architecture. *Plant Physiol* **156**, 832–843. (doi:10.1104/pp.111.173856)
122 Wittwer, J. W. 2011 Excel solver examples. See http://www.vertex42.com/ExcelArticles/excel-solver-examples.html.
123 Pasquet-Kok, J., Creese, C. & Sack, L. 2010 Turning over a new 'leaf': multiple functional significances of leaves versus phyllodes in Hawaiian *Acacia koa*. *Plant Cell Environ.* **33**, 2084–2100. (doi:10.1111/j.1365-3040.2010.02207.x)
124 Vico, G. & Porporato, A. 2008 Modelling C_3 and C_4 photosynthesis under water-stressed conditions. *Plant Soil.* **313**, 187–203. (doi:10.1007/s11104-008-9691-4)
125 Meidner, H. & Mansfield, T. A. 1968 *Physiology of stomata*. Maidenhead, UK: McGraw-Hill.
126 Dubbe, D. R., Farquhar, G. D. & Raschke, K. 1978 Effect of abscisic acid on the gain of the feedback loop involving carbon dioxide and stomata. *Plant Physiol.* **62**, 413–417. (doi:10.1104/pp.62.3.413)
127 Aasamaa, K. & Sõber, S. 2011 Stomatal sensitivities to changes in leaf water potential, air humidity, CO_2 concentration and light intensity, and the effect of abscisic acid on the sensitivities in six temperate deciduous tree species. *Environ. Exp. Bot.* **71**, 72–78. (doi:10.1016/j.envexpbot.2010.10.013)

GLOSSARY

A	net rate of leaf photosynthetic CO_2 assimilation
BSC	bundle sheath cells
CA	carbonic anhydrase
CAM	crassulacean acid metabolism
CCM	carbon-concentrating mechanism
DC	decarboxylase enzymes
E	actual rate of leaf transpiration
g_s	leaf stomatal conductance to water vapour
K_{leaf}	hydraulic conductance of leaves
K_{plant}	whole-plant hydraulic conductance
K_{stem}	stem hydraulic conductance
MC	mesophyll cells
PACMAD	acronym for the lineage of grasses comprising the subfamilies Panicoideae, Arundinoideae, Chloridoideae, Micrairoideae, Aristidoideae and Danthonioideae
PAR	photosynthetically active radiation
PEPC	phosphoenolpyruvate carboxylase
PET	potential evapotranspiration
PPFD	photosynthetic photon flux density
RH	relative humidity
Rubisco	ribulose-1,5-bisphosphate carboxylase/oxygenase
VPD	vapour pressure deficit
WUE	leaf water-use efficiency (A/E)
Ψ_{leaf}	leaf water potential